

BRNO UNIVERSITY OF TECHNOLOGY
VYSOKÉ UČENÍ TECHNICKÉ V BRNĚ

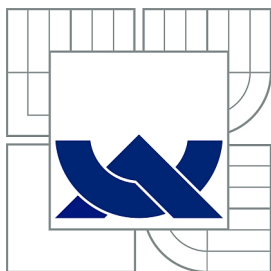
FACULTY OF MECHANICAL ENGINEERING
INSTITUTE OF SOLID MECHANICS, MECHATRONICS AND
BIOMECHANICS
FAKULTA STROJNÍHO INŽENÝRSTVÍ
ÚSTAV MECHANIKY TĚLES, MECHATRONIKY A BIOMECHANIKY

DESIGN AND IMPLEMENTATION OF TESTING DEVICE
FOR SPECIMEN MECHANISM FOR ELECTRON
MICROSCOPE

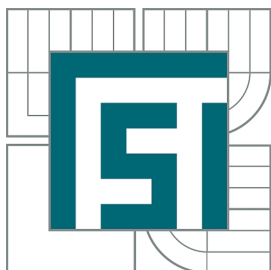
MASTER'S THESIS
DIPLOMOVÁ PRÁCE

AUTHOR
AUTOR PRÁCE

Bc. TOMÁŠ TRNKÓCY



BRNO UNIVERSITY OF TECHNOLOGY
VYSOKÉ UČENÍ TECHNICKÉ V BRNĚ



FACULTY OF MECHANICAL ENGINEERING
INSTITUTE OF SOLID MECHANICS,
MECHATRONICS AND BIOMECHANICS

FAKULTA STROJNÍHO INŽENÝRSTVÍ
ÚSTAV MECHANIKY TĚLES, MECHATRONIKY A
BIOMECHANIKY

DESIGN AND IMPLEMENTATION OF TESTING DEVICE FOR SPECIMEN MECHANISM FOR ELECTRON MICROSCOPE

NÁVRH A REALIZACE TESTOVACÍHO ZAŘÍZENÍ MANIPULAČNÍHO
MECHANISMU VZORKU PRO ELEKTRONOVÝ MIKROSKOP

MASTER'S THESIS
DIPLOMOVÁ PRÁCE

AUTHOR
AUTOR PRÁCE

Bc. TOMÁŠ TRNKÓCY

SUPERVISOR
VEDOUCÍ PRÁCE

doc. Ing. JIŘÍ KREJSA, Ph.D.

BRNO 2013

Vysoké učení technické v Brně, Fakulta strojního inženýrství

Ústav mechaniky těles, mechatroniky a biomechaniky

Akademický rok: 2012/2013

ZADÁNÍ DIPLOMOVÉ PRÁCE

student(ka): Bc. Tomáš Trnkócy

který/která studuje v **magisterském navazujícím studijním programu**

obor: **Mechatronika (3906T001)**

Ředitel ústavu Vám v souladu se zákonem č.111/1998 o vysokých školách a se Studijním a zkušebním řádem VUT v Brně určuje následující téma diplomové práce:

Návrh a realizace testovacího zařízení manipulačního mechanismu vzorku pro elektronový mikroskop

v anglickém jazyce:

Design and implementation of testing device for specimen mechanism for electron microscope

Stručná charakteristika problematiky úkolu:

Práce se zabývá návrhem a implementací testovacího zařízení pro manipulační mechanismus vzorku v elektronovém mikroskopu. Testovací zařízení a jeho software zajišťuje měření několika parametrů mechanismu, jejich statistické vyhodnocení a porovnání se specifikací.

Cílem je vytvořit komplexní testovací zařízení s jednoduchým uživatelským rozhraním, s požadavkem náhrady stávajícího nemodulárního a nestabilního řešení a jeho rozšíření o testování dalších parametrů. Tím bude zajištěno zkrácení výrobní doby nových mechanismů.

Cíle diplomové práce:

1. Proved'te rešeršní studii stávajících testovacích procedur mechanismu
2. Navrhněte řešení odečítání potřebných veličin pro jednotlivé testy
3. Vytvořte jednoduché uživatelské prostředí pro testovací procedury v prostředí LabView
4. Implementujte statistické vyhodnocení naměřených dat pro jednotlivé procedury
5. Otestujte nové testovací zařízení

Seznam odborné literatury:

1. Marsh, Eric R.: Precision spindle metrology, Destech Publications, Inc., ISBN 978-1-60595-003-7
2. Moore, Wayne R.: Foundations of mechanical accuracy, Moore Special Tool Co., 1970, ISBN 9780262130806

Vedoucí diplomové práce: doc. Ing. Jiří Krejsa, Ph.D.

Termín odevzdání diplomové práce je stanoven časovým plánem akademického roku 2012/2013.

V Brně, dne 8.1.2013

L.S.

prof. Ing. Jindřich Petruška, CSc.
Ředitel ústavu

prof. RNDr. Miroslav Doupovec, CSc., dr. h. c.
Děkan fakulty

ABSTRACT

This thesis deals with design and implementation of a testing device for a specimen mechanism in electron microscope. The testing device and its software provides measuring of important parameters of the mechanism, their statistical evaluation and confrontation with specification. The aim is to build complex test tool with simple user interface in order to replace the old and unstable version and its extension with new tests.

KEYWORDS

Electron microscope, stage, linear encoder, capacitive sensor, LabView

ABSTRAKT

Práce se zabývá návrhem a implementací testovacího zařízení pro manipulační mechanismus vzorku v elektronovém mikroskopu. Testovací zařízení a jeho software zajišťuje měření několika parametrů mechanismu, jejich statistické vyhodnocení a porovnání se specifikací. Cílem je vytvořit komplexní testovací zařízení s jednoduchým uživatelským rozhraním, s požadavkem náhrady stávajícího nemodulárního a nestabilního řešení a jeho rozšíření o testování dalších parametrů.

KLÍČOVÁ SLOVA

Elektronový mikroskop, manipulační mechanismus, lineární enkodér, kapacitní senzor, LabView

TRNKÓCY, Tomáš *Design and implementation of testing device for specimen mechanism for electron microscope*: master's thesis. Brno: Brno University of Technology, Faculty of mechanical Engineering, Institute of solid mechanics, mechatronics and biomechanics, 2013. 67 p. Supervised by doc. Ing. Jiří Krejsa, Ph.D.

DECLARATION

I declare that I have elaborated my master's thesis on the theme of "Design and implementation of testing device for specimen mechanism for electron microscope" independently, under the supervision of the master's thesis supervisor and with the use of technical literature and other sources of information which are all quoted in the thesis and detailed in the list of literature at the end of the thesis.

Brno

.....

(author's signature)

ACKNOWLEDGEMENT

I would like to thank to everyone who helped me with professional advice and guidance as well as my family and friends who supported me.

CONTENTS

List of symbols, physical constants and abbreviations	9
1 Introduction	10
2 Microscopy principles	11
2.1 Electron microscope	11
2.2 Stages	13
2.3 110x110mm stage mechanics	14
3 Testing procedures	17
3.1 Smallest step	18
3.2 Repeatability	19
3.3 Drift test	20
3.4 Linear and rotation test, reversal method	21
3.4.1 Rotation test	22
3.4.2 Linear test	24
4 Testing equipment	25
4.1 Capacitive sensor	25
4.1.1 Principle	25
4.1.2 Used capacitive sensor and accessories	26
4.2 Linear encoders	27
4.2.1 Principle	28
4.2.2 Used linear encoders	28
4.3 PC Software and hardware	29
4.3.1 MPC and microscope server software	29
4.3.2 NYCe4000	32
5 Building the test tool hardware and application	33
5.1 Mechanical parts	33
5.1.1 Capacitive sensor holder and base	33
5.1.2 Linear artifact and supports	34
5.1.3 Rotation artifact	36
5.2 LabView - Controlling the stage	37
5.3 LabView - Main VI	39

5.4	LabView - Tests	43
5.4.1	Rotation precision test	43
5.4.2	Linear precision test	48
5.4.3	Repeatability test	51
5.4.4	Smallest step test	53
5.4.5	Drift test, Burn-in test	54
5.5	Test tool verification and evaluation	56
6	Conclusion	60
	Bibliography	61

LIST OF SYMBOLS, PHYSICAL CONSTANTS AND ABBREVIATIONS

UI User interface

VI Virtual instrument

MPC Microscope PC

TEM Transmission electron microscope

SEM Scanning electron microscope

AC Alternate current

PWM Pulse width modulation

DAQ Data acquisition

NI National Instruments

1 INTRODUCTION

As we live in 21st century often called information age or computer age, the human knowledge has come on by leaps and bounds. We are keen to know more and more about the world around us and we try to penetrate into the essence of things and principles happening in the nature. During the last few decades electron microscopy has experienced huge growth as with its help we can delve into the subnanometer world. There scientists observe atomic structures of the materials, examine biological samples with precision never seen before or they can produce microchips within nanometer dimensions.

This thesis deals with testing of the important part of the scanning electron microscope - the stage, particularly the 110mm stage. As there are high requirements for accuracy and precision of the mechanism movement, several tests need to be performed on manufacturer site before delivering the stage to FEI Company and before final implementation into the microscope, to ensure that system meeting the specifications will be delivered to the customer.

Nowadays, the manufacturer of the 110mm stages tests newly built ones with an old application, which quite often exhibits instability such as crashing the testing application or loosing the measured data. Therefore the testing of the stages takes disproportionately long time as the test procedures has to be repeated multiple times. The aim of this thesis is to build a new application in LabView environment. It has to fully substitute the existing one, has to be user friendly and stable. In addition, new tests should be implemented to extend its functionality.

This thesis will describe bases of electron microscopy and moving of the sample in the scanning electron microscope. Then the particular stage type will be introduced together with procedures to test its important parameters. Programming of the testing procedures in LabView environment will be shown as well as the designed and manufactured mechanical parts needed for measurement. Finally, the new testing application will be evaluated and implemented on the manufacturer site.

2 MICROSCOPY PRINCIPLES

2.1 Electron microscope

First electron microscope has been patented in year 1931 by Ruska and Knoll and was capable of four-hundred-power magnification [1]. Today, electron microscopes have reached resolutions of better than 0.05nm, more than 4000 times better than a typical light microscope. The difference between the optical and electron microscope is that optical one magnifies small objects by means of visible light and with an assembly of glass lenses, while electron microscope uses beam of electrons to increase resolution and magnification. The process of focusing of the beam is almost the same but lenses used in electron microscope are electromagnetic. Also the electron beam has to be in vacuum as the electrons cannot travel appreciable distances in the atmospheric pressure.

Generally we distinguish between two types of microscopes - transmission electron microscope (TEM) and scanning electron microscope (SEM). The TEM was the first electron microscope to be developed. It works by shooting a beam of electrons at a thin slice of a sample and detecting those electrons that make it through to the other side. The TEM lets us look in very high resolution at a thin section of a sample. This makes it particularly good for learning about how components inside a cell, such as organelles, are structured. SEM lets us see the surface of three-dimensional objects in high resolution. It works by scanning the surface of an object with a focused beam of electrons and detecting electrons that are reflected and knocked out from the sample surface. At low magnifications, entire objects (such as insects) viewed on the SEM can be in focus at the same time.

The schematics principle of SEM and TEM are illustrated in figure 2.1.

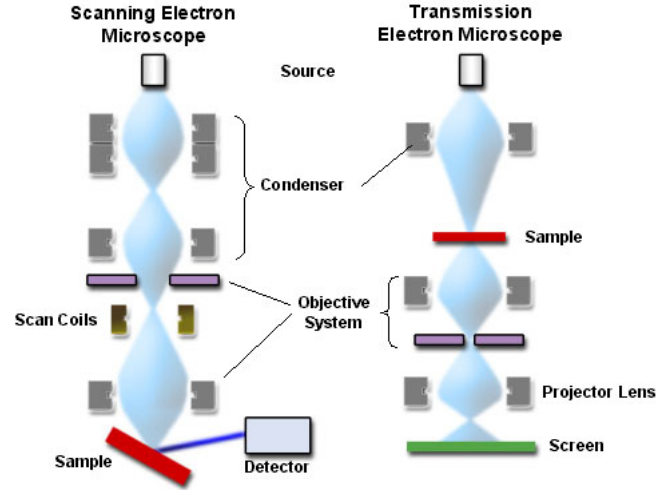


Fig. 2.1: SEM and TEM microscope principle [2]

Besides those two types of microscopes also Focused Ion Beam microscopes (FIB) can be found on the market. Instead of electron beam the ion beam is used. As the ions are many times more massive than electrons they sputter away atoms from the specimen surface when they impapact. The ion beam can be scanned over the surface to obtain an image or can be controlled to locally expose the sample to the beam as for example used in i-beam lithography.

Nowdays FEI company produces all of the mentioned microscope types from the low-end sector to the hi-end.



Fig. 2.2: Examples of the FEI Company portfolio [3]

Also other types such as AFM microscopes (Atomic Force Microscopy) can be found on the market, yet FEI Company does not produce them. The AFM microscope consists of cantilever with sharp tip, which scans the surface of the specimen. When the tip is in close proximity of the surface, the cantilever bends due to mechanical contact force, van der Waals forces, capillary forces etc. The deflection of the cantilever is then measured usually with laser beam which is reflected into an array of photodiodes.

2.2 Stages

To precisely position the specimen under the electron beam, sophisticated mechanism is needed. Generally the stage moves with the specimen in five degrees of freedom - it lineary moves along X, Y and Z axis, rotates around R and Tilt axis.

Usually linear axes on the stages move in high precision linear guides, but they are actuated in different manners. While the ultra-high precision stages are actuated by piezomotors and their position is scanned by linear encoder, on low cost systems actuation is performed by means of threaded lead screw accompanied with rotary encoder. Needless to say that the first approach is more expensive yet more precise as we can achieve precision within units of nm.

FEI Company distributes several types of stages. From the 50x50mm stage driven by DC motors for low end microscope group, up to the ultra high resolution 100x100mm stage driven by ultra-sonic piezo motors for the high end group. Besides those mentioned, FEI Company also provides other stages depending on the customer needs.



Fig. 2.3: 50x50mm stage driven by DC motors



Fig. 2.4: 100x100mm stage driven by piezo motors

2.3 110x110mm stage mechanics

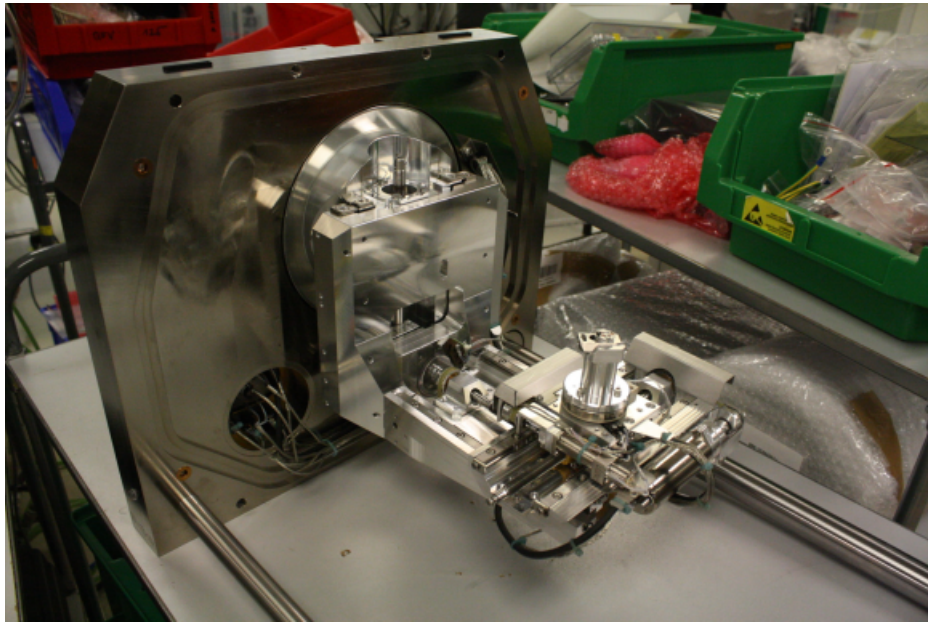


Fig. 2.5: The 110x110mm stage assembled

As mentioned in chapter 1 this thesis deals with testing particular stage type in scanning electron microscope - the 110x110mm stage (fig.2.5). Expression 110x110mm stands for movement range in X and Y axis.

Let's describe the RY unit shown in figure 2.6 first. An enclosed DC motor (1) drives a worm via flexible coupling (2) and belt drive (3). The worm rotates the gearwheel directly connected to the rotation table (4). The angular position of the rotation table is determined by rotary encoder (5) mounted on the worm shaft and its zero position by index switch (6).

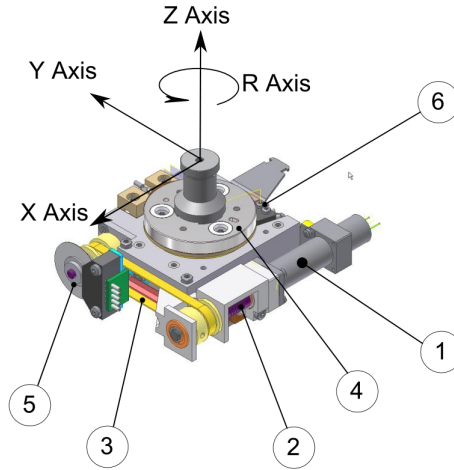


Fig. 2.6: RY unit

Y axis unit consist of RY unit carriage, encapsulated DC motor and lead screw. The RY unit slides thanks to linear bearing in RY carriage (8). Actuation is performed by enclosed DC motor (9) which rotates lead screw (10) by the belt drive. Position of RY unit is determined by rotary encoder mounted directly on the lead screw. All parts mentioned above slide on X carriage (11) and are actuated in the X axis direction on the same principle as the Y axis. Whole X carriage than can be moved in Z axis direction and tilted around tilt axis, which is parallel to the X axis. The tilt axis is the eucentric axis. That means that if the area of interest on the specimen lies on the eucentric axis, there is no need to refocus the electron beam when the specimen is tilted.

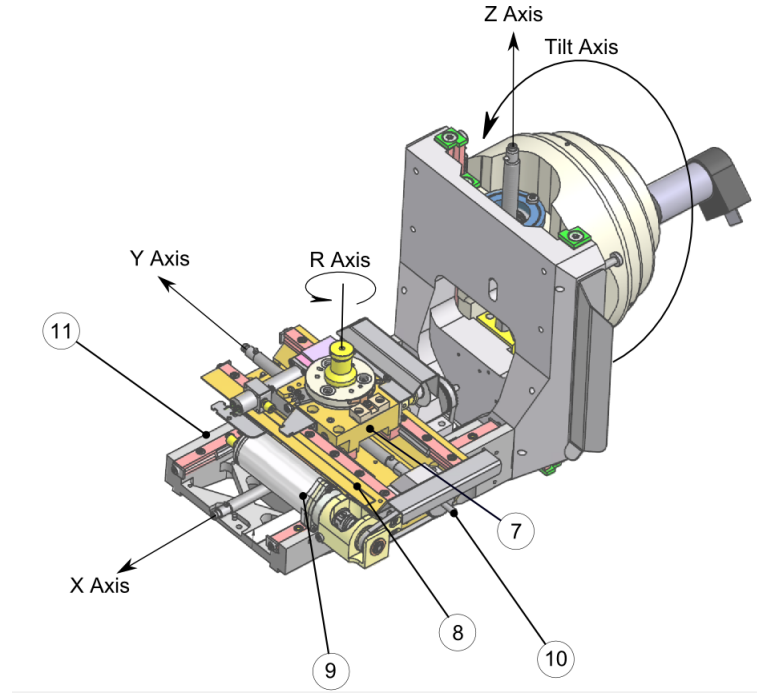


Fig. 2.7: X unit

In table 2.1 is summary of 110x110mm stage parameters as specified in FEI documentation. Each of the parameter will be discussed in next chapter.

	X	Y	Z	R	T
Usable travel					
Maximum speed					
Smallest step					
Repeatability					

Tab. 2.1: Specification for 110mm stage

3 TESTING PROCEDURES

Existing test tool software has been put on supplier site during development phase of the 110x110mm stage. Prior the delivery to final assembly in Brno the stage has to be tested and adjusted at the manufacturer site and has to pass several tests. The table 3.1 shows that in year 2012 the number of delivered stages almost doubled since the previous year and it is expected that in year 2013 the number of stages to be delivered will be even higher.

2010 - Q4	x
2011	x
2012	x
2013 - Q1	x

Tab. 3.1: Number of stages delivered in particular years

Quite huge amount of time is spent with final testing the stage at manufacturer site. When the stage is delivered to factory in Brno and implemented into a newly assembled microscope it is tested again right in real operation mode. The table 3.2 shows the issues gathered from the FEI's quality database. Those issues are caused either by not well designed testing procedure, or some of the parameters are not even tested on the manufacturer site. When such a issue occurs, the stage has to be readjusted or send back to the manufacturer. According to the table 3.2 the most often issue is that the stage does not meet the specification for the repeatability. The repeatability parameter is inevitably connected with the adjustment of the X and Y axis bearing. If the testing procedure to check the bearing setting will be improved, those issues can be eliminated to the minimum. Another problem which often occurs is the drift issue. As this parameter is not tested by the manufacturer, new testing procedure will be implemented into the new testing application. Other mechanical issues mean, that for example after the delivery some of the screws on the stage are not tightened or even some parts are missing. This is of course a serious issue, but it is out of the scope of this thesis.

ISSUE	COUNT
repeatability	x
drift	x
contamination	x
X, Y axis bearing	x
smallest step	x
rotation	x
other mechanical	x

Tab. 3.2: Stage issues

As the existing test tool software is still in the development version and has never been optimized, it exhibits unstability, in means that for example it crashes in the middle of the test and all measured data are lost, it was necessary to either fix the test tool application or make a new one from scratch. The old version is written in Matlab scripts with almost no documentation at all, so it was decided to build the new one in LabView environment as it provides better scalability and modularity. In addition it was decided to implement few new tests. The aim was to provide stable, user friendly test tool to the manufacturer so that it is possible to test the stages in shorter time, yet more precisely so that the number of the issues could be decreased.

In next chapters will be mentioned existing testing procedures and the new ones to be implemented will be described.

3.1 Smallest step

During the assembly of the stage it is necessary to tune the position of linear bearings and the lead screw to assure that the stage moves sufficiently freely yet with no play. To reveal any disturbances in stage's movement, the smallest step test has been proposed. The name of the parameter is self-explaining - it says if the stage is able to repeatedly perform smallest step possible according to the specification listed in table 2.1. The test is performed for X and Y axis in five locations and five lead screw positions for each axis, where location means the distance on the lead screw and the position of the lead screw means its rotation. It is necessary to perform the test in all locations to assure that the linear bearings are mounted as parallel as possible, so the carriage is not squeezed during its movement. To check that the lead

screw is not crookedly mounted, the smallest step test is executed in five 90°-spaced positions on each location. Not correctly aligned lead screw can cause hysteresis in the stage's movement.

The test flows: Stage moves to first location and settles for a while. Then a step of 250nm is performed. What is measured is the real displacement of the axis sensed by linear encoder. Final position of the previous step is taken as an initial position for next one. Then it goes in the same manner 10 steps of 250nm forward and 10 steps backward. When the sequence of 20 steps is finished, lead screw rotates 90 degrees and whole procedure starts again. Test continues until the smallest steps are measured at all 5 positions (0°, 90°, 180°, 270°, 360°) and at all five locations (-50mm, -25mm, 0mm, 25mm and 50mm) on the lead screw. The stage passes the test when 95% of the results are equal or less than 250nm as the specification says.

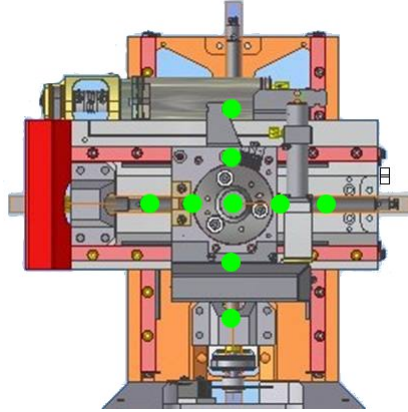


Fig. 3.1: Locations on each axis where the smallest step is measured

3.2 Repeatability

We distinguish between two types of repeatability - unidirectional and bidirectional. While the unidirectional represents the ability of the stage to return to a given point from the same previously defined point, the bidirectional represents the ability of the stage to return to a given point coming from a random previous point. The repeatability test is performed simultaneously for X and Y axis and the value specified is the mean value of an error plus three-times standard deviation of many moves from random directions to the same point. The results are evaluated for both axes separately.

Bidirectional repeatability is the one of the most concerned issue within the stage testing. Quite common is the situation when user saves the location with an

interesting feature on the specimen. The stage must be able to precisely return to that location after it has been moved in any direction. To test if the stage meets specification following procedure has been proposed.

The stage is tilted to 0 degrees to neglect the effect of the possible drift and X and Y axis are centred. From this initial position $[X,Y]=[0,0]$ stage moves to point with coordinates $[8\text{mm},8\text{mm}]$ and back to initial position. What is measured is the displacement in X and Y axis between the initial position and the position when the movement is finished. To satisfy the bidirectional repeatability condition another 15 moves with different X and Y coordinates are performed. Figure 3.2 shows all 16 moves and their order.

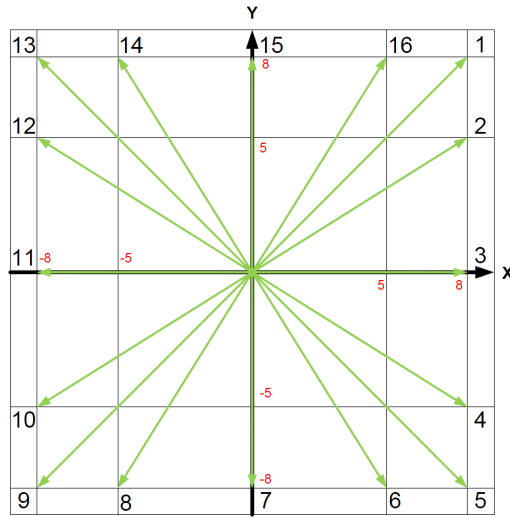


Fig. 3.2: Repeatability moves [9]

3.3 Drift test

This so called drift test relates to the Y axis while using the stage for the TEM sample preparation. TEM preparation is an automatic routine that creates lamella out of the bulk material, which is then used in TEM microscopy. The procedure follows: The stage positions the location of interest. Than it tilts to 52 degrees and I-beam starts cutting away material such that a thin lamella results. During the procedure which can take up to 1 hour it must be ensured that the drift in Y axis is within the specification, so that the automated software based on image recognition can keep up following the lamella pattern.

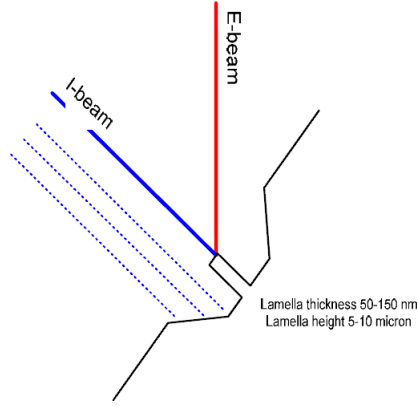


Fig. 3.3: TEM lamella preparation [4]

3.4 Linear and rotation test, reversal method

As mentioned in the introduction to this chapter, new tests became required, namely the X and Y axis linear test and the rotation precision test. The linear test ensures that the linear bearings for the X and Y axis are mounted precisely, that they are not bended or pre-stressed too much, so the stage's movement is linear with the displacement in perpendicular direction within the specification limits. Similar tests are also performed on the UHR stage with measurement system called LARA. However, due to the significant dimension differences between the UHR stage and the 110mm stage LARA cannot be used. So that it would be necessary to build a new one to accommodate 110mm stage which would be expensive, and its cost would never be justified according to the price of the stage. Therefore it was necessary to come up with more simple and less expensive solution to measure required parameters. The reversal method offers great method to achieve this goal relatively cheaply and with minimum of equipment.

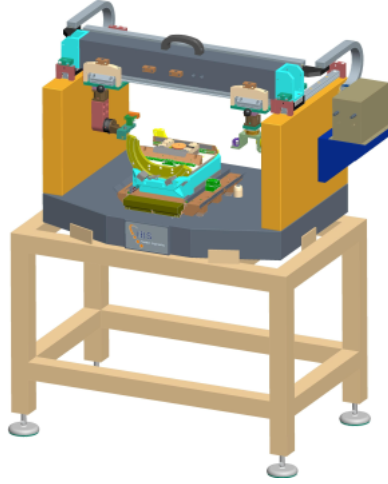


Fig. 3.4: LARA measurement system for UHR stage [8]

Every measurement consists of a combination of the value being measured and a residual. If the residual can be measured as well, it can be subtracted from the measurement to obtain desired value. One of the method to estimate the residual is to measure a known artifact. But manufacturing for example precise linear artifact with almost perfect straight edge is expensive as can be seen on LARA example. Therefore so called "self-calibration techniques" [6] are often used in straightness or spindle measurements.

One of the most popular self-calibration method is the reversal method. It relies on the symmetry to eliminate the contribution of the artifact to the measurement. In next two sections an application of the reversal method to the linear and rotation test for our purpose will be shown.

3.4.1 Rotation test

Purpose of the rotation precision test is to ensure that RY unit (fig.2.6) is correctly assembled and that the rotation table axis rotates within the specification. Test is performed by radially measuring the distance between rotation artifact and capacitive sensor firmly mounted on the RY unit base. The artifact turns during the test as it is mounted on the rotation table and capacitive sensor stay still. What the displacement sensor sees while the R axis turns is a combination of the artifact error and rotary table motion error. To separate these two types of error, reversal method enters the scene.

Figure 3.5 shows the forward and reverse setup for the Donaldson reversal method [5].

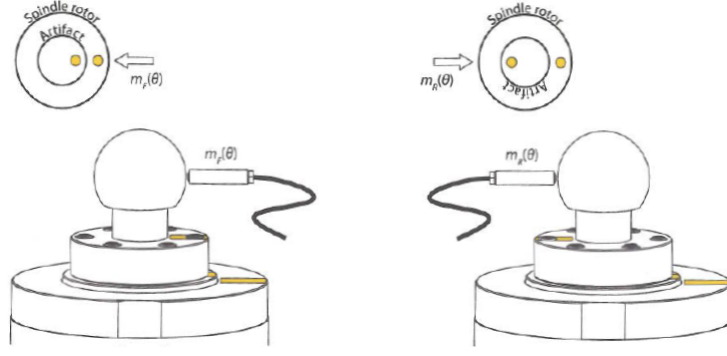


Fig. 3.5: Setup for forward (left) and reverse (right) spindle measurement [7]

In forward direction setup the artifact, displacement sensor and rotation table are aligned and measurement for complete revolution m_F is taken. It can be expressed as combination of rotation table's motion error S and the roundness error of the artifact R :

$$m_F = R + S \quad (3.1)$$

In the reverse direction the displacement sensor and artifact are rotated 180° while the position of the rotation table stays untouched. Therefore the rotation table motion error reverses sign:

$$m_R = R - S \quad (3.2)$$

Adding equations 3.1 and 3.2 we can isolate the artifact roundness profile (eq.3.3) while subtracting those equations results in motion error profile (eq.3.4).

$$R = \frac{m_F + m_R}{2} \quad (3.3)$$

$$S = \frac{m_F - m_R}{2} \quad (3.4)$$

It must be emphasized that components of m_F and m_R have to correspond to the same angular location.

The unprocessed measured data of several revolutions of the spindle can be divided into three main features. The first is a fundamental component. As the artifact will never be perfectly centred on the axis of rotation, the sensor sees this eccentricity as a once per revolution sine wave. This fundamental component is not considered as an error in radial measurement, as it can be removed in post processing. Second feature is a synchronous error which is a polar plot of error motion components having frequencies that are integer multiples of the rotation frequency. The synchronous error polar plot is created by averaging the values at

corresponding angular locations through all revolutions. If the synchronous component is subtracted revolution by revolution from the raw data, the asynchronous component remains.

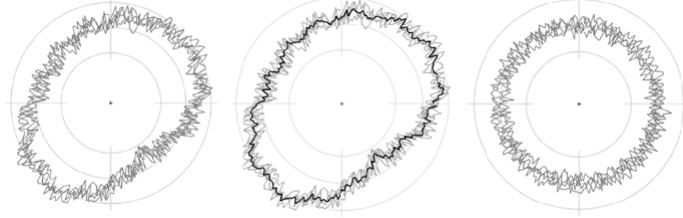


Fig. 3.6: Graphical illustration of raw data, synchronous and asynchronous error [7]

3.4.2 Linear test

The linear test is designed to check that linear bearings for X and Y axis are properly setup and movement in perpendicular direction to the axis is within the specifications. Also this test detects hysteresis for both axes. The test is lineary analog to the Donaldson reversal method. Linear artifact is used and opposite to the rotation test, the artifact stays still and the displacement sensor slides along the straight edge. Expressions for evaluating the straightness profile of the artifact and the linear motion error of the axis remain in the same form as 3.3 and 3.4.

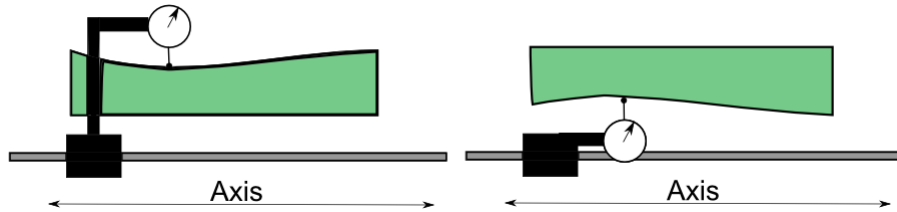


Fig. 3.7: Setup for forward (left) and reverse (right) linear measurement

4 TESTING EQUIPMENT

In previous chapter we have described each of tests performed on the stage. To obtain desired measurement data it was necessary to decide which instrument will be used to gather this data. In next chapters will be described which measurement device was used for each of the tests and its characteristics.

4.1 Capacitive sensor

4.1.1 Principle

The principle of non-contact distance measurement with the capacitive sensor is based on the principle of the parallel plate capacitor. For conductive targets, the sensor and the target form the two plate electrodes. The capacitance of idealized parallel plate capacitor C is directly proportional to the surface area A of each plate, the electric field permittivity of free space ϵ_0 and the relative permittivity of the insulator between the plates ϵ_r . The capacitance C is inversely proportional to the distance d between the plates.

$$C = \epsilon_0 \cdot \epsilon_r \cdot \frac{A}{d} \quad (4.1)$$

However, this expression is only first order approximation since it neglects fringe effects, therefore in practice this relationship is realized by designing the sensors as guard ring capacitor (fig.4.1).

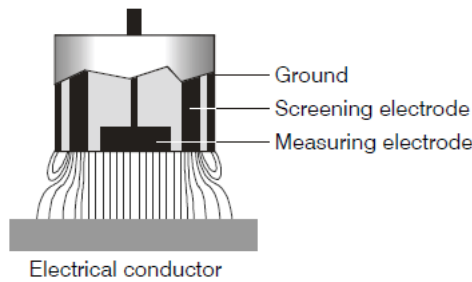


Fig. 4.1: Scheme of guard ring capacitor [10]

If a constant AC current flows through the sensor, the amplitude of the AC voltage at the sensor is proportional to the distance between the capacitor and the metal target. The AC voltage is demodulated, amplified and output as an analog signal.

4.1.2 Used capacitive sensor and accessories

In order to measure rotational precision of the R axis and linear precision of X and Y axis, Micro Epsilon capaNC DT 6100 single channel system with capacitive sensor CS02 was purchased.



Fig. 4.2: CapaNCDT 6100 controller [11]

The CS02 sensor with measuring range 0.2 mm is connected through the sensor cable to the controller which is powered by 24V DC. Analog output signal from controller in range between 0 and 10 volts is then connected to the analog input on the NI DAQ card. Worth to mention that due to the sensor construction and measuring principle the analog output from the controller is linear with proposed linearity of 0.3% FSO (full scale output)[11]. The output linearity is valid when measuring flat targets. But with cylindrical targets there are significant measured value deviations e.g. due to the concentration of the field lines at the highest point or a capacity increase due to a larger measuring spot. Therefore while measuring such a surface the controller indicates more then the real distance is. This effect is calculated by the manufacturer and corresponding characteristic must be implemented in the measuring software.

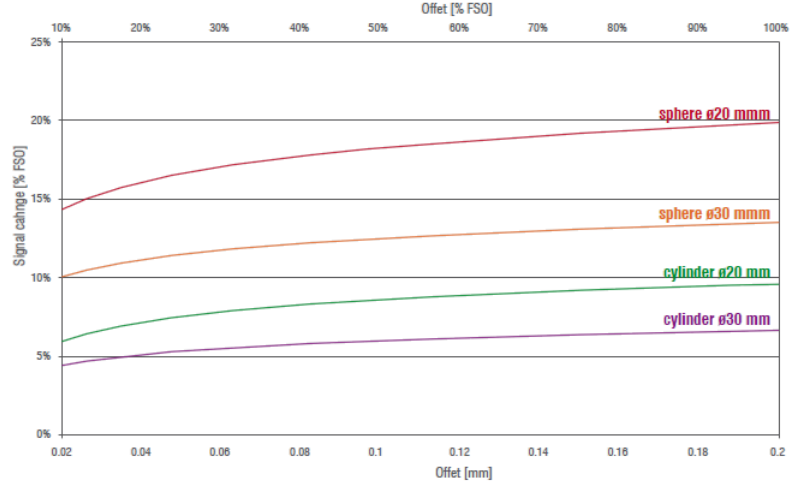


Fig. 4.3: Signal change for various target geometries for CS02 sensor[11]

4.2 Linear encoders

In order to read actual position of the X and Y stage axis two linear encoders are used - one for each axis. Reason why position is read from linear encoder and not directly from the rotary encoders already mounted is the play and friction in the motion chain. As the rotary encoder is mounted directly on the lead screw the play in the motor and gearbox is eliminated. However there is still play between the lead screw thread and nut and play in linear bearings. The linear encoders are mounted at the end of the motion chain therefore readings from them are actual stage positions and any change displacement is visible in the image.

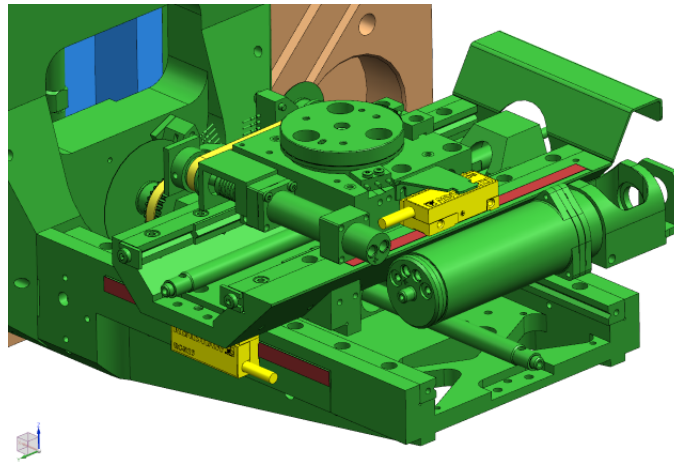


Fig. 4.4: Placement of the linear encoders for X and Y axis

4.2.1 Principle

Linear encoder systems usually consists of three parts – the scale, the readhead and the interpolator. An infra-red LED in the readhead projects light onto the several scale facets, which reflects it back onto an index grating. The combined effect of the scale's periodic pattern and index grating's pattern produces two sinusoidal interference signals on the photodetector in the readhead. These signals are 90° phase shifted and fed into the interpolator which generates standard TTL quadrature output.

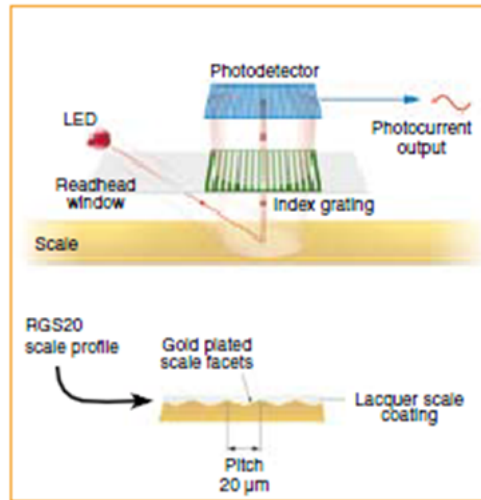


Fig. 4.5: RG2 optical scheme [12]

4.2.2 Used linear encoders

For the purpose of our test tool readhead RGH25F, 20μm pitch scale and interpolator REF0400 was purchased, one set for each axis. In this setup we are able to measure axis position with precision of 50nm. The quadrature output is read by NI DAQ card discussed later.



Fig. 4.6: Readhead RGH25F, RG2 20µm pitch scale, interpolator REF0400 [12]

4.3 PC Software and hardware

Whole testing application was developed on the prototype of the motion test tool assembled for the Research and Development department purposes. It is equipped with microscope chamber including the 110mm stage, power source, the Bosch Rexroth NYCe4000 motion control system and the MPC (Microscope PC).



Fig. 4.7: Motion test tool at FEI R&D

4.3.1 MPC and microscope server software

Microscope PC is a standard standalone PC running Windows XP operating system. It accommodates microscope server software which controls whole microscope, such as stage movement, electron and ion beam, vacuum pumps and other features of the microscope.

For controlling the stage a simple application called TAD is available in the microscope software (fig.4.8). Through TAD the movement of the stage is controlled and position of each axis are read. Also the testing procedures can be called from the selection list. When talking about controlling the movement of the stage, it is good to point out that the stage can move in different modes as Vaške thoroughly explained in his diploma thesis [9]: *"Every stage can move in three modes based on the way it is controlled. First one is movement in open loop when voltage is directly applied to a motor without feedback. This mode is used only for some special diagnostic procedures. The second is so called jog. In this case a stage runs in speed control mode when speed information is differentiated from position. The last mode is point-to-point motion. Here the desired value represents position. However, PID for position control is slow with great integrate constant to be as precise as possible so a stage starts motion in speed control mode and when it is close to the desired position, controller is switched to position control."*

Another important type of movement is a homing procedure. As the stage uses relative encoders it is necessary to find out the zero position to set-up a coordinate system. In case of rotation axis the zero position is determined by the microswitch acting as an index point. The X, Y and Z axis determines the zero position by reaching hard-end stop. The axis moves in speed control mode and when it reaches the hard-end it stops and drop in velocity is detected. The position of stage is then taken as a lower (or higher) limit and consequent positions are then determined from the encoder. Finally, the tilt axis zero position is detected by the inductive proximity sensor and a sensor flag.

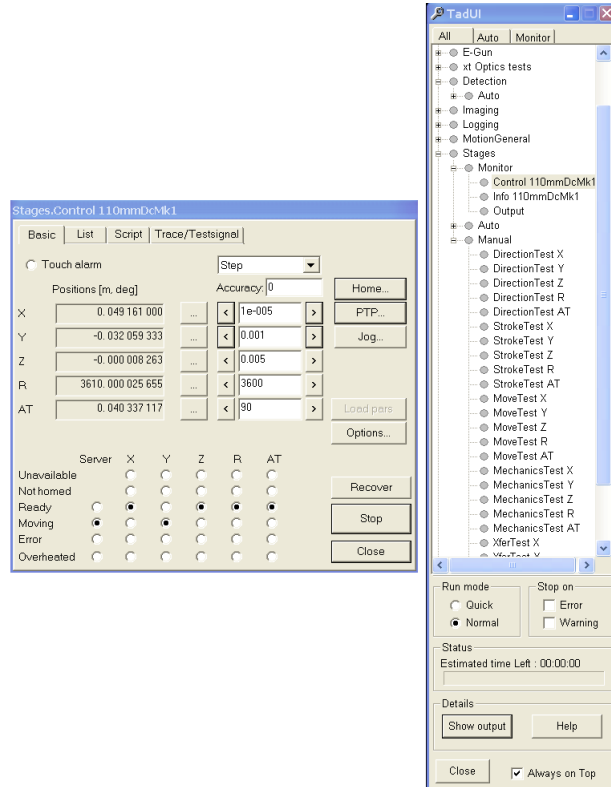


Fig. 4.8: TAD

The MPC is also equipped with the data acquisition card PCI-e 6320 from the National Instruments Company. This card provides readings from linear encoders through the 32-bit counter input and from the capacitive sensor through the 16-bit analog input. This card has been chosen as it can be flawlessly implemented into the LabView development environment installed on the MPC in version 2012.

Finally the MPC communicates through the firewire connection with the NYCe4000 motion control system in order to perform stage movements.

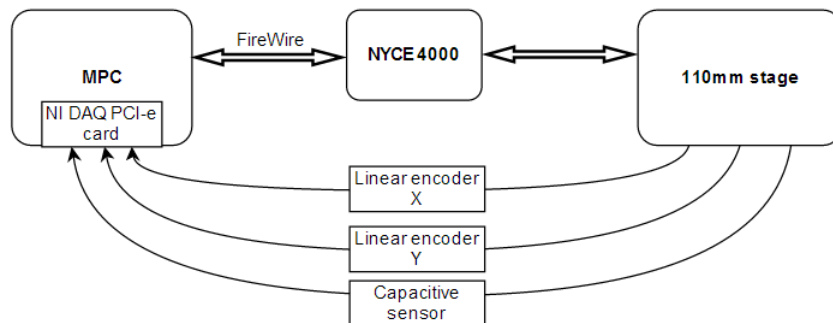


Fig. 4.9: Test tool connection scheme

4.3.2 NYCe4000

In order to implement extremely precise and steady stage control the modular motion controller NYCe4000 [13] developed by the Bosh Rexroth Company is used within almost all FEI Company's microscope systems. NYCe4000 system for controlling the 110mm stage consists of backplane equipped with plug-in motion control unit NY4110 which communicates through the firewire connection with MPC and can control up to 10 axes. To control all five axes of the stage the NY4125 low power five axis PWM drive module is used. The other two modules seen on figure 4.10 are NY4130 DC drive modules which can control brushed DC motor by directly applying the voltage instead of the PWM principle. These modules are used to control the aperture system connected to the motion test tool, yet it is out of the scope of this thesis.



Fig. 4.10: NYCe4000 motion controller

5 BUILDING THE TEST TOOL HARDWARE AND APPLICATION

5.1 Mechanical parts

5.1.1 Capacitive sensor holder and base

In order to properly mount the capacitive sensor onto the stage the CS02 Sensor Holder has been designed. Its purpose is to firmly hold the CS02 sensor and its cable in small assembly. This prevents damaging the sensor or unplugging the cable during manipulation between measurements. The position of the sensor in relation to the holder is adjustable with set screw, however when properly set it is not necessary to adjust the working distance between the sensor and the target. Whole sensor holder sits on two pins on the base and is tightened with the screw.

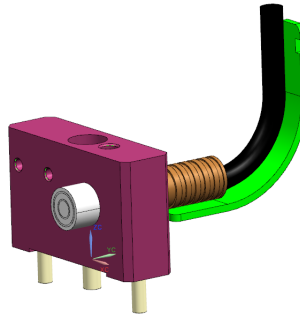


Fig. 5.1: Capacitive sensor holder assembly

Base bracket is designed to be mounted on the top of RY-module of the stage and it serves to accommodate sensor holder. Emphasis was placed on the variability of the base. Thanks to that, it can be used as for the linear measurement so for the rotation measurement. Center of the base has been hollowed to make enough space for R-artifact. Sensor holder can be placed in 4 different positions on the base. This prevents the stage to be damaged between the measurements by repeatedly changing the position of the sensor. All possible positions of the sensor holder are illustrated on the figure 5.2. Figure 5.3 shows all previously discussed parts fabricated and assembled.

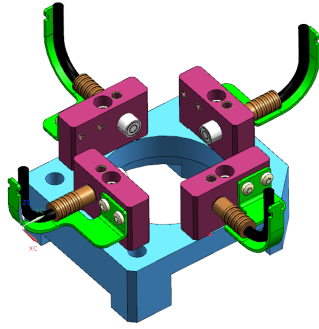


Fig. 5.2: Capacitive sensor base with all possible sensor positions

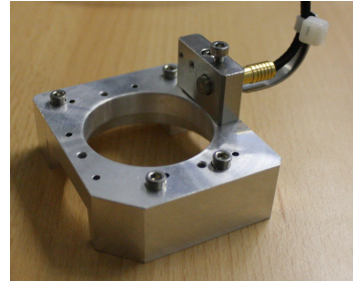


Fig. 5.3: Base with capacitive sensor holder

5.1.2 Linear artifact and supports

As previously proposed in chapter 5.18 great advantage of this method is no need for ultra precise straightedge. On this basis relatively cheap straightedge has been designed and manufactured. From 220mm long, 30mm wide and 15mm high stainless steel block has been milled out with several relief holes and one side of the straightedge has been abraded to achieve straightness of 0.01mm. This so called linear artifact is mounted with two shoulder screws onto the supports. These supports were fabricated by laser sintering technology which delivers light and stiff mechanical parts with low cost and in extremely short time. Quotation for same parts made from aluminium was three times more expensive and estimated delivery time was more than ten-times longer. Also the weight factor had to be taken in mind. The supports are made of glass filled Polyamide PA 3200 which is more than twice lighter than aluminium. Although it is possible to cut threads to this polyamid material it was decided to use aluminium press nuts for shoulder screw which hold linear artifact as it is expected that the threads will be heavily stressed by repeatedly mounting and dismounting the artifact.

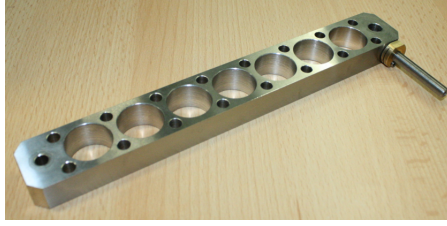


Fig. 5.4: Linear artifact

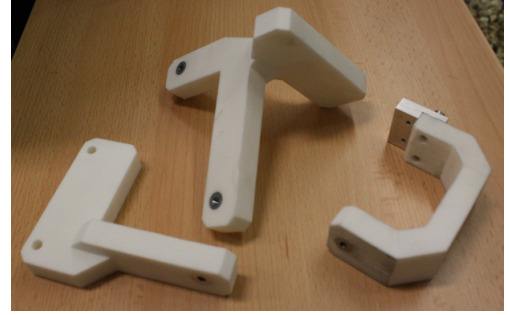


Fig. 5.5: Supports for linear artifact

Important part of the linear artifact is the adjustment screw seen in figure 5.4. As the supports will never be properly mounted onto the Z carriage of the stage due to the manufacturing tolerances, the linear artifact's straightedge will hardly be parallel to the measured axis. With the adjustment screw it is possible to very gently settle the artifact to be as parallel as needed for the measurement. Shoulder screw on the left side of the artifact (according to fig.5.4) acts as pivot point. The adjustment screw with ultra fine pitch (100 threads per inch) pushes against the second shoulder screw while tightened causing the artifact to turn around the pivot point. On the opposite side of the adjustment screw is spring plunger which eliminates the play. The whole mechanism of adjusting the artifact illustrates figure 5.6.

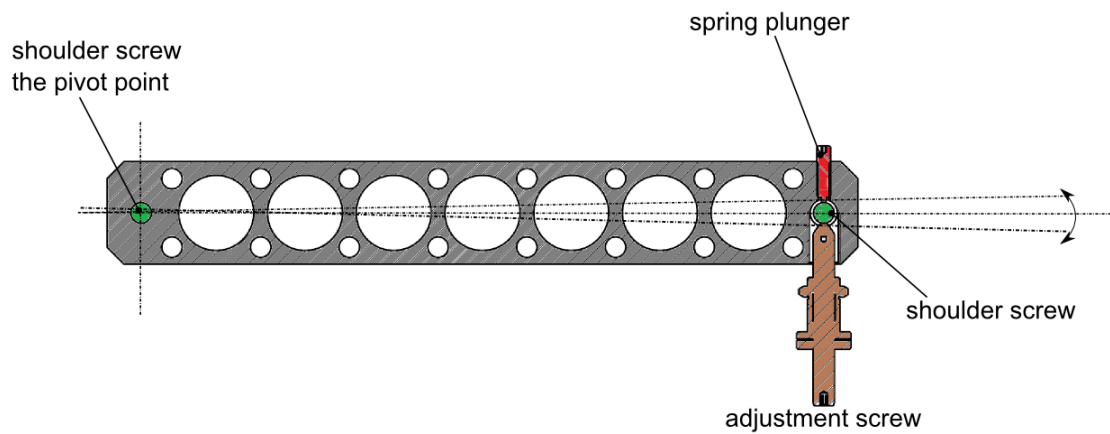


Fig. 5.6: Linear artifact adjustment mechanism

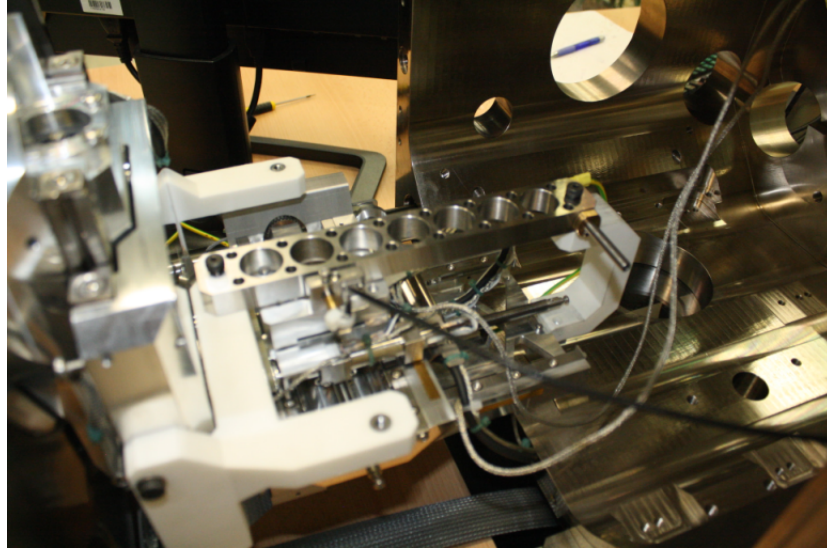


Fig. 5.7: Setup for linear measurement on X axis

5.1.3 Rotation artifact

The same approach in relation to the artifact precision considering the Donaldson reversal method applies for the rotation artifact. This artifact is 45mm high cylinder with diameter $\phi 30\text{mm}$. Two dowels at bottom side serve to precisely position the artifact onto the rotation table. Their position corresponds with position of the hole and groove on the table therefore the artifact can be mounted just in two ways - the one direction and exactly 180 degrees opposite direction. Thus this is ideal system for the reversal method. Finally the artifact is pressed onto the table by the tightening knob running through the hole in the center of the artifact. The whole setup for rotation measurement can be seen in figure 5.9. The rotational artifact sits on the rotation table and is held in position by the tightening knob. Capacitive sensor bracket and holder are mounted on the RY unit.



Fig. 5.8: Rotational artifact and tightening knob

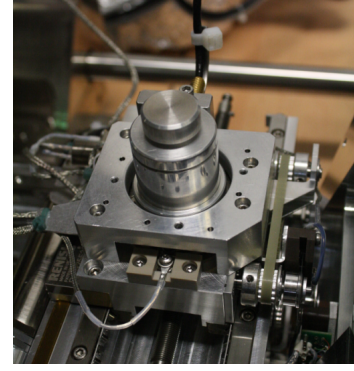


Fig. 5.9: Rotational measurement setup

5.2 LabView - Controlling the stage

First step in developing the testing application was to gather data from the microscope server software and access them from the LabView environment. We are talking about reading the axes positions, axes states as well as controlling the stage movement. Natural choice was to use the same approach as Vaške used in his work [9] in means of using the XTLib, which is dynamic link library developed to grant access to microscope instruments for third party developers. Unfortunately during the development of the LabView application several problems occurred. Namely, it is not possible to read out the axes states, axes error reports and home axes independently. Last issue was found out during the rotation precision test programming. The XTLib can move the rotation axis only in range $-\pi$ to π . If greater value than π is provided to the movement command, the axis rotates only for the given value of degrees minus the whole multiples of π . Of course this could be bypassed by calling the movement command several times, but this approach causes the stage to stop for a while between the commands which is not desired behaviour. Therefore it has been decided to connect directly to the HAL motion layer.

In order to access and control the motion instrument of the xTserver from LabView it is necessary to connect to the MdlMotionServer. To do that, *MdlConnectionServer* constructor node through MdlMotionHepler library is called with input parameter *sConnectionServer*. When done, an invoke node *CreateConnection* establishes connection to the microscope server. After successful connection another constructor node *MdlMotionServer* is called followed by invoke node *initialize* which accesses the property *iMotServer* containing the properties needed to read the stage

status, such as axes positions, states etc. LabView diagram processing all above mentioned is saved in `Microscope_connect.vi` and can be seen in fig.5.10

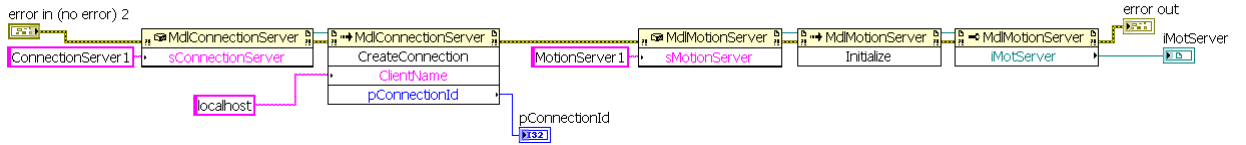


Fig. 5.10: Connection to the MotionServer in LabView

When the connection to the MdlMotion block is established it is possible to read the stage states through calling the *AxesState* property of the MotionServer. State of each axis can become to one of 9 possible values: *Not Homed*, *Error*, *Unavailabe*, *Ready*, *Homing*, *Moving*, *Jogging*, *Overheated*, *Open Loop*. Those states are represented in form of boolean value which indicates if the specific axis is available to perform the movement and into the text information describing the state. The axes positions are obtained through *Position* property of the MotionServer. All the stage states and positions are read continuously during the timeout event in producer loop (which will be described later) while the test application runs and are distributed through global variables wherever these values are needed. Whole LabView scheme can be seen in fig.5.11.

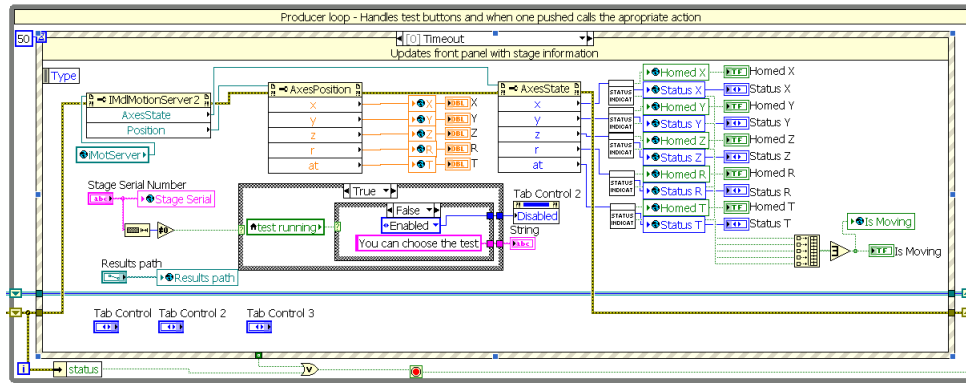


Fig. 5.11: Reading the stage states in LabView

Calling the StartMotion method serves to move with the stage. Before calling this method, the motion descriptor has to be initialized. In here we can set which axis should move, where to, with which speed and in which mode. First parameter to set is the axis mask. Each axis is represented by unique integer number, specifically the X axis = 1, Y=2, Z=4, R=8, Z=16. By adding those numbers we can determine

which of the axes will move. For example, if we want to move with X and Y axis, the value for the axis mask will be 3. As name of the parameters AxesPosition and AxesVelocity suggests, here the final position and speed can be set. The last parameter called Type distinguishes how the stage will move, whether in point-to-point mode, jog or open loop mode as described in chapter 4.3.1. When the motion descriptor is filled in the StartMotion method is called and the stage moves. This method also returns the MotionID value which uniquely describes just performed movement and it can be served for the StopMotion method which stops the identified movement. Whole LabView scheme can be seen in fig.5.12.

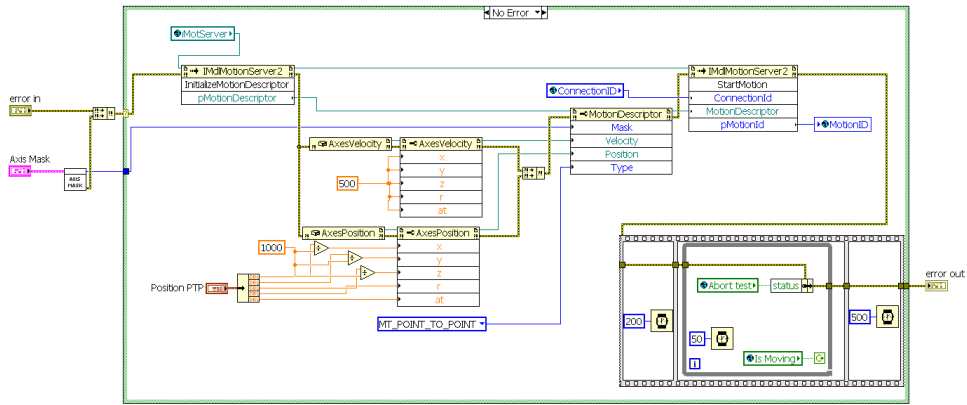


Fig. 5.12: Moving the stage in point to point mode in LabView

5.3 LabView - Main VI

What the user sees right after he starts the application is so called Main UI. It consists of panel which controls the stage similarly to the TAD software UI (fig.4.8), buttons and controls to select and set tests and area where selected test's UI pops-up. Front panel of the **Main.vi** illustrates default appearance of the UI right after the start (fig.5.13). When no test is selected, the user can control the stage through the LabView TAD, after some of the tests is initiated all controls from the UI are disabled and control of the stage is taken over the called test, yet all the indicators of the axes states and positions are still updated throughout the testing procedure.

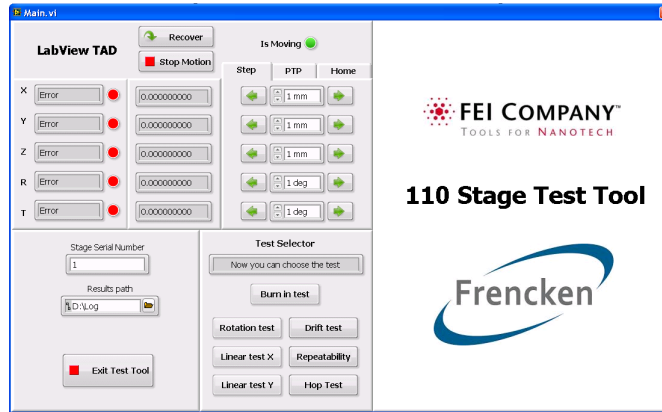


Fig. 5.13: Main UI of the test tool application

Block diagram of the Main UI is based on the queued state machine design pattern. It consists of two loops - the producer loop adds states to process into the queue which is then processed in consumer loop acting as a state machine. In our case the producer loop is an event case structure. It reacts to the change of value of the specific button on the front panel, so it runs only when an event occurs and does not consume any processor resources when waiting for an event. The case structure can be also initialized with timeout value. It means that if no event from buttons or other controls occurs, the timeout case runs at rate specified by timeout value port. The timeout case in our application updates the front panel with the axes states and positions every 50 milliseconds. When the button from the test selector (see fig.5.13) area is pressed, the event case associated with it runs, adding the specific state into the queue. The queue is then processed with the consumer loop acting as a state machine. When any state is inserted into the queue, the while loop executes the case according to the state which is at the first position of the queue and then it waits for another state to process. In the consumer loop we are basically calling individual tests and controlling behaviour of the front panel. The great advantage of the producer-consumer design pattern is its scalability. By simply editing the queue elements list more states can be easily implemented in order to for example extend the application with another test. To better understand the data flow in the block diagram of the `Main.vi` an example of calling the Drift test will be shown:

First of all the queue is initialized by inserting the name of the queue and the element data type into the *Obtain Queue* block. The element data type is the list of all possible states, for our purpose it means list of all tests and *Initialize*, *Re-init after test*, *Init before test*, *Exit* states. Then we try to connect to the motion server through the `Microscope_connection.vi`. If the connection is not successfully es-

established the application pops-up an error warning and stops.

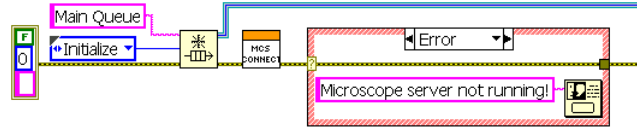


Fig. 5.14: Initializing the queue

Now the application is in idle state waiting for any event to occur. When for example the Drift Test button is pressed the event structure case associated with it executes, adding the *Init before test* and *Drift Test* states into the queue. It is then processed in the consumer loop.

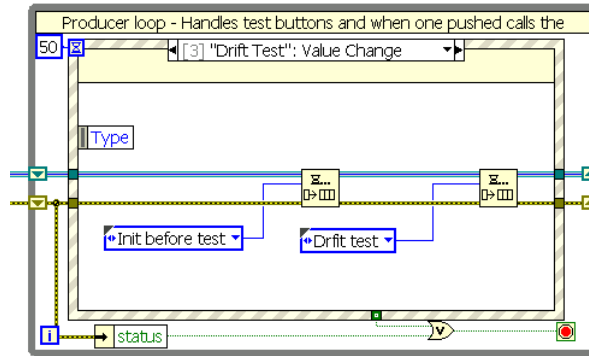


Fig. 5.15: Adding elements into the queue - producer loop

First element in the queue is the *Init before test* state which disables all controls of the front panel to ensure that no button can be pressed and any user interaction will be possible only with the test window which will appear. When the disabling routine is finished, the consumer loop processes the next state - the *Drift Test*. It opens the test UI in the subpanel on the Main VI front panel and waits until the testing procedure is finished. When so, it enqueues the *Re-init after test* state into the queue which closes the test UI and enables all front panel buttons again.

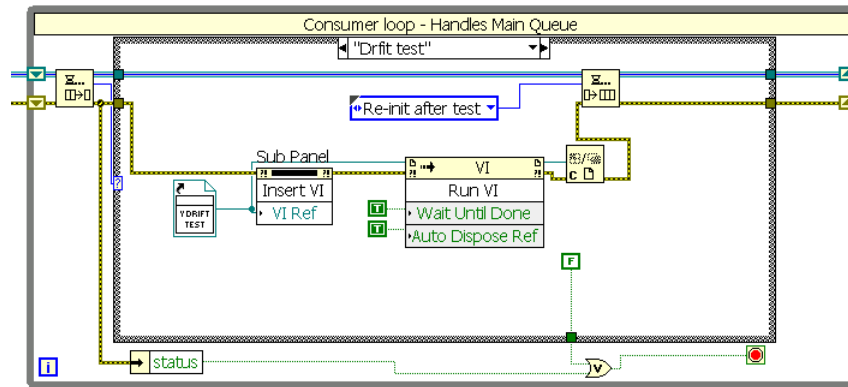


Fig. 5.16: Calling the test VI - consumer loop

The whole `Main.vi` block diagram is shown in fig.5.17. It can be seen that it consists of producer and consumer loop. In the middle there is also another event case structure for the purpose of controlling the stage through the LabView version of TAD. It principally works the same as the producer loop, yet it does not influence the queue, so it was decided to create the TAD control as a separated event structure which is disabled when any of the test is called.

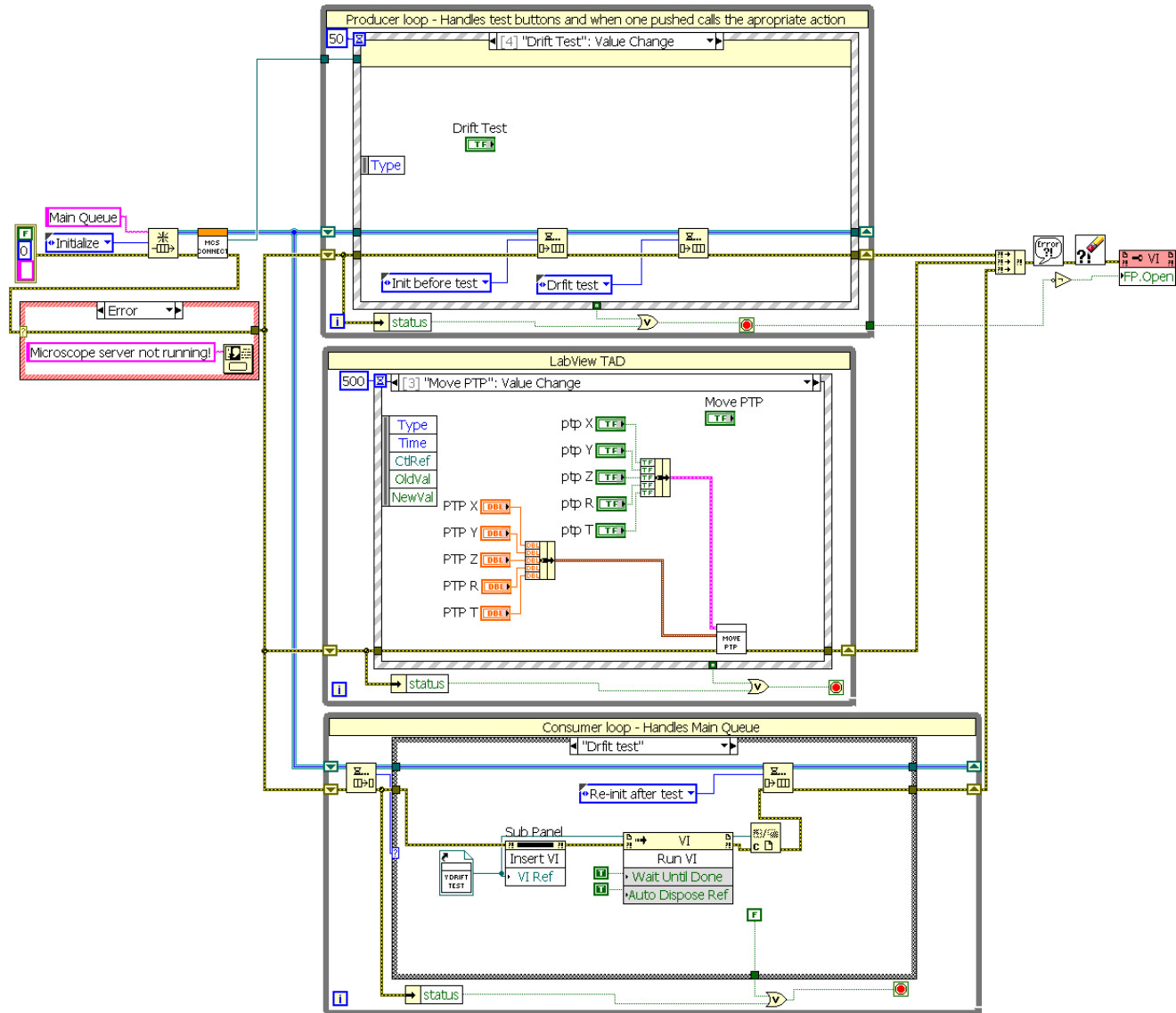


Fig. 5.17: Complete block diagram for Main.vi

5.4 LabView - Tests

5.4.1 Rotation precision test

The rotation precision test VI is based on the same programming design as the Main VI - the queued state machine pattern. Producer loop handles the states of the buttons on the front panel and timeout event updates the front panel with data from capacitive sensor when the test is started. The test is separated into the several states and the test flow follows the pattern illustrated in figure 5.19.

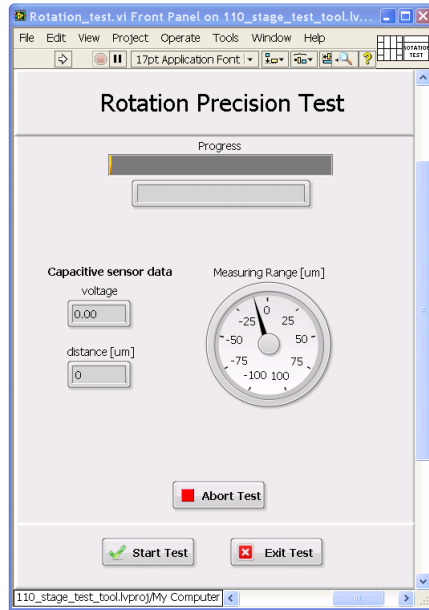


Fig. 5.18: UI for rotation test

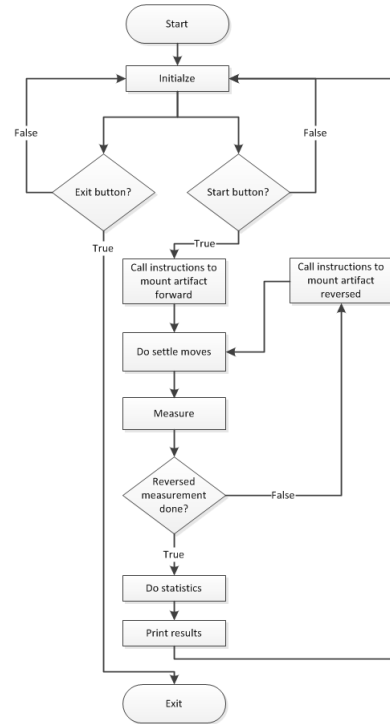


Fig. 5.19: Flow diagram for rotation test

When the test is initialized from the Main UI it enters the *Initialize* state in consumer loop first. In this state all variables are initialized to the default value and the state machine waits for user interaction such as pressing the start or exit button. When the start button is pressed, the producer loop inserts the *Start* state into the queue and consumer loop processes this state in means that it disables the start and exit button and fills in the queue with test states which are consequently processed.

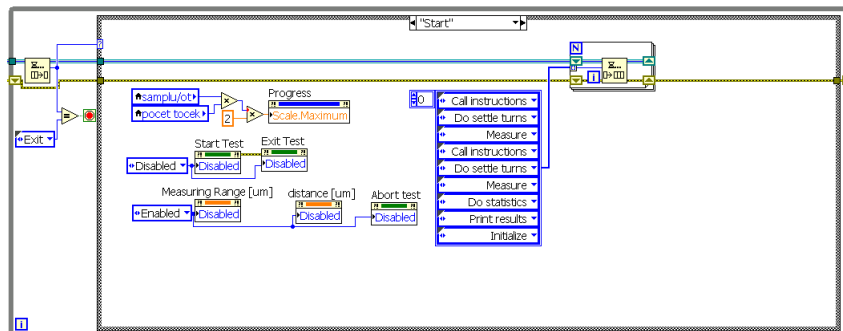


Fig. 5.20: Filling in the queue with test procedures

Call instructions state - in this state small window with an instruction for the user how to mount the rotation artifact onto the rotation table pops-up. During mounting the artifact so called touch alarm can be detected. Touch alarm event occurs when any part of the rotation table - which is on different potencial from the ground - touches any part of the microscope chamber. Then the current flow is sensed by the safety mechanism and it automatically stops any movement of the stage to prevent for example damaging the lenses. If the touch alarm is detected, the stage must be recovered from the error state by pressing the Recover button.

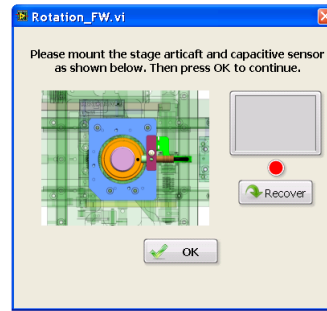


Fig. 5.21: Instruction window

Do settle moves state - here the rotation axis homes, then performs 5 consequential revolutions to settle the rotation mechanism, as during the mounting the artifact significant stress can be applied to the gears which will never occur during normal operation. Then the stage homes again and moves to initial position at 0° .

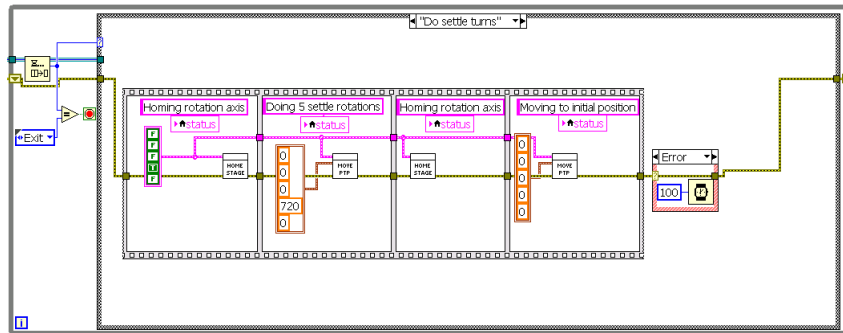


Fig. 5.22: *Do settle moves* state

Measure state - when settling is done the rotation axis performs 10 revolutions and the data from capacitive sensor are gathered. A sample from capacitive sensor is taken at every 25th tick of rotation encoder. According to the worm wheel gear ratio the encoder provides 46250 ticks per one revolution of rotation table. Therefore

at each revolution 1850 samples of equally distributed data from capacitive sensor is saved in memory for further processing.

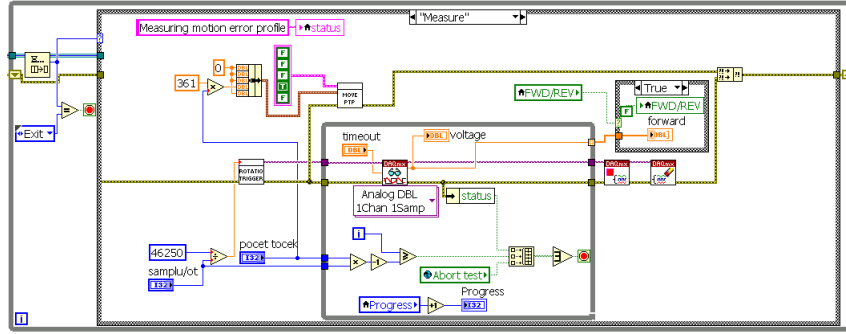


Fig. 5.23: *Measure* state

Do statistics state - after the measurement for forward setting is finished the whole mounting, settling and measuring procedure runs again for the reversed setup. The acquired data are in form of voltage and as mentioned in chapter 4.1.2 the voltage output from capacitive sensor controller must be compensated according to the characteristics provided in [11]. This characteristic is in form of an image, therefore it was necessary to extrapolate this information into an equation. The characteristic spline for 30mm cylindrical shape (fig.4.3) has been transformed to the array of points and the polynomial interpolation through those points has been performed to obtain the polynomial coefficients. With this information the distance can be calculated directly with the equation:

$$x[\mu m] = 1.271 \cdot 10^{-6} \cdot U_{out}^4 - 3.822 \cdot 10^{-5} \cdot U_{out}^3 + 0.000437 \cdot U_{out}^2 + 0.01747 \cdot U_{out} - 0.006215 \quad (5.1)$$

As the artifact will never be mounted precisely centered the measured data will contain a fundamental component in form of sine wave which has to be removed. Therefore the best sine wave is extrapolated from the measurement and subtracted from the original data.

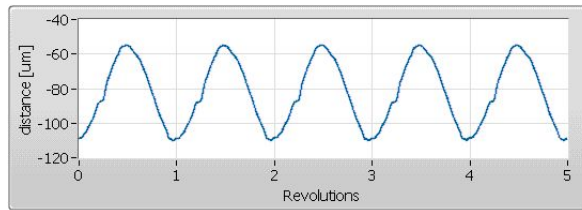


Fig. 5.24: Raw measured data

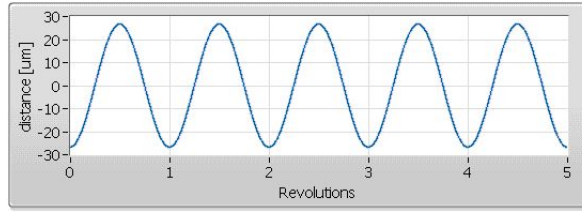


Fig. 5.25: Best sine fit extrapolated from raw measurement

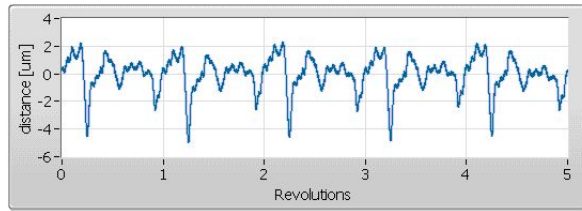


Fig. 5.26: Raw displacement - sum of motion and artifact error

To obtain a synchronous error, the mean value at corresponding radial locations is computed. As described in chapter 3.4.1 the synchronous error is a sum of motion error and artifact profile error. So the forward and backward measurements are processed according to the equations 3.3 and 3.4 and polar plot of the motion error profile and the artifact profile are printed as well as the radial error is computed as a difference between the maximum and minimum value of the synchronous error dataset.

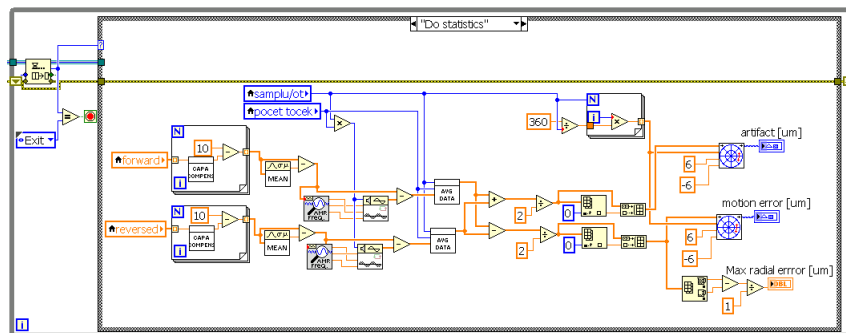


Fig. 5.27: *Do statistics* state

Print results state - all the results from the test are printed into an html report page containing the resulted polar plots and value of maximal radial error. The report clearly says if the stage passed the test and is enclosed to the stage packaging.

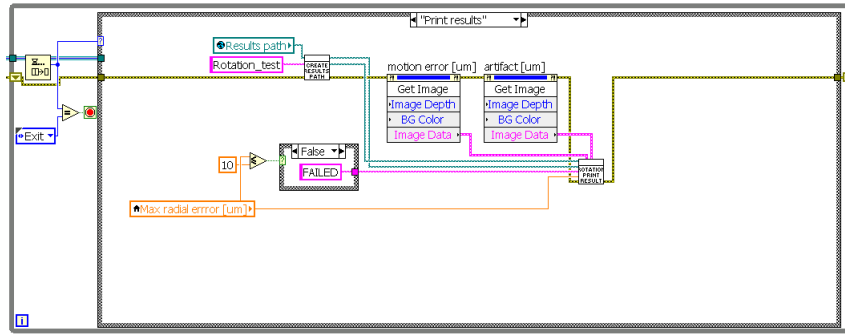


Fig. 5.28: *Print results* state

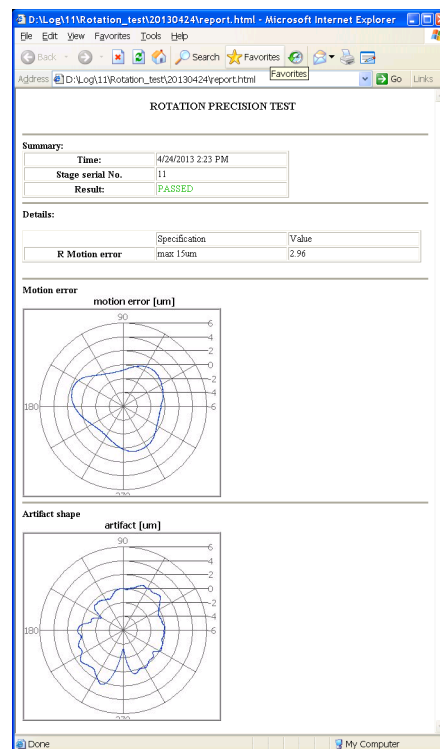


Fig. 5.29: Rotation test html report

5.4.2 Linear precision test

Linear precision test for X and Y axis is a linear variation for the rotational test with few small differences. As usual, after the test is called, initialized and started, the queue is filled in with sequence of states. First, the user is prompted by message window to dismount any accessories from the stage. Then the stage moves to safe distance so the linear artifact and capacitive sensor can be mounted according to the instructions which pops-up in window called in *Mount artifact* state. When the

artifact and sensor is mounted, user acknowledges this by pressing the OK button and the stage moves the capacitive sensor approximately two millimeters close to the artifact near the position of pivot point of the linear artifact (fig.5.6). Then the *Approach artifact* state occurs. The stage is making steps of $20\text{ }\mu\text{m}$ closer to the artifact in a while loop until the measured distance between the artifact and sensor is approximately 0.1mm, which is the center of measuring range of the capacitive sensor.

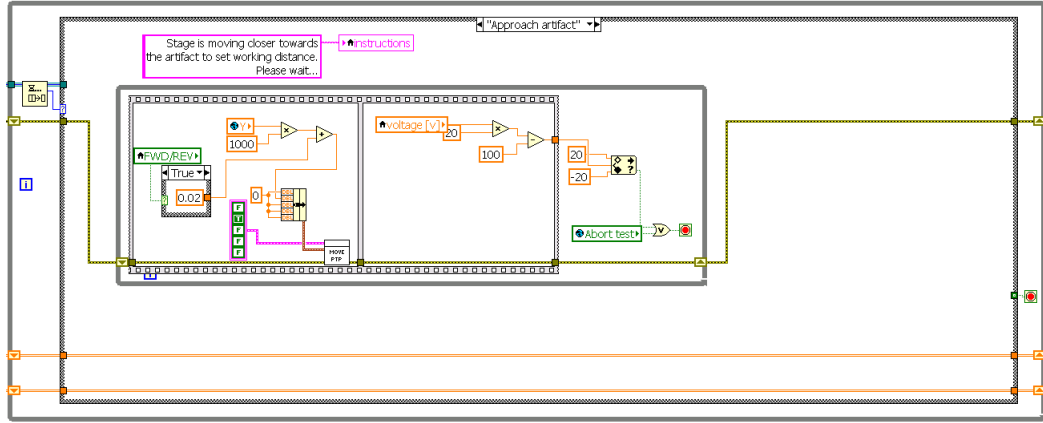


Fig. 5.30: Approaching the linear artifact

When the sensor is on the position, the loop stops and the stage moves to the opposite side of the artifact through the *Calibrate* state. During the movement another loop continuously checks if the capacitive sensor is not moving too much closer to the artifact. If so, the dialog window is shown to instruct user to adjust the linear artifact to prevent sensor from damage and the calibration state runs again. When the stage successfully makes it to the opposite end of the artifact, the user has to adjust the linear artifact with setting screw to move to right position indicated by the gauge indicator on the UI. When set, user presses the Set button and whole procedure runs once more to ensure that the distance of the capacitive sensor and the linear artifact is within the measuring range of the sensor across the whole range of the axis. Once the linear artifact is set to the right position, the stage makes 10 moves to the left and 10 moves to the right. During each movement 1100 equally distributed samples from capacitive sensor are taken. Because the linear artifact will never be mounted directly parallel to the axis, there will be a slope visible in measured data. To remove this misalignment from the measurement, the end point fit method has been used. The equation of the misalignment line U_{slope} starting at

the first measurement point and ending at the last point has to be found:

$$U_{slope} = m \cdot X + x_0 \quad (5.2)$$

where

misalignment m is expressed as $m = \frac{u_n - u_0}{n}$

n is number of samples from the capacitive sensor

u_n is the voltage measured at the last measurement point

u_0 is the voltage measured at the first measurement point

Then the true straightness error can be calculated as

$$U_{real} = U_{measured} - U_{slope} \quad (5.3)$$

To represent the voltage in a distance form the following equation is used

$$x[\mu m] = U_{real} \cdot \frac{MR[\mu m]}{10[V]} \quad (5.4)$$

where

MR is the measuring range of the capacitive sensor in μm

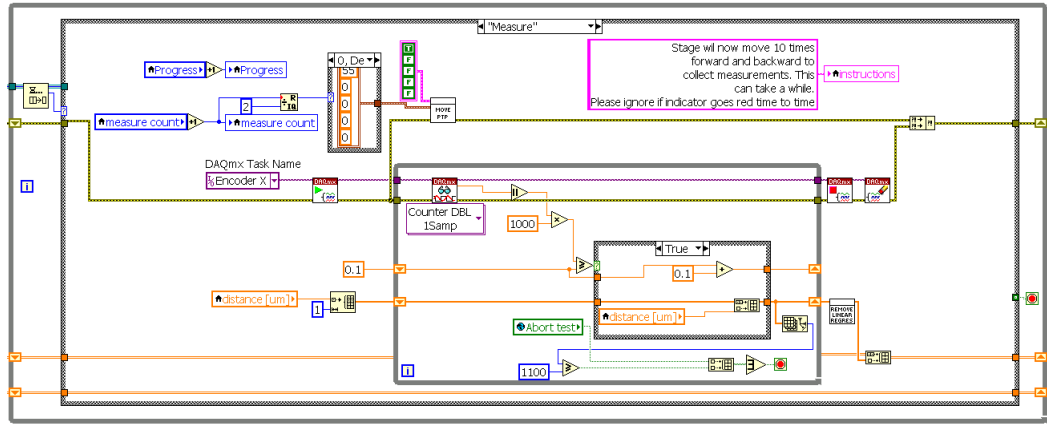


Fig. 5.31: *Measure* state

When the measurement data are gathered for the forward setting, again the instruction window opens to show how the user has to mount the artifact and capacitive sensor for the reverse setup and whole approaching, calibrating and measuring procedure runs again. In *Process data* state the gathered data are separated to four arrays - two arrays for forward setup and two for reversed setup. First array in each setup represents motion when the stage travels from left to the right and

second array represents the opposite motion. For each motion the motion error L is calculated by equation

$$L = \frac{m_F + m_R}{2} \quad (5.5)$$

where

m_F is measurement in forward setup

m_R is measurement in reversed setup

The maximum motion error value is then calculated and matched with specification. Graphs showing progress of the motion error are then printed into an html report in *Print results* state.

5.4.3 Repeatability test

The VI for the repeatability test (chapter 3.2) follows the flow diagram shown in fig.5.33. As all the test VIs are programmed on the same queued state machine pattern, they share basically the same producer loop which controls the UI and updates the front panel. Only difference is in number of states and their purpose.

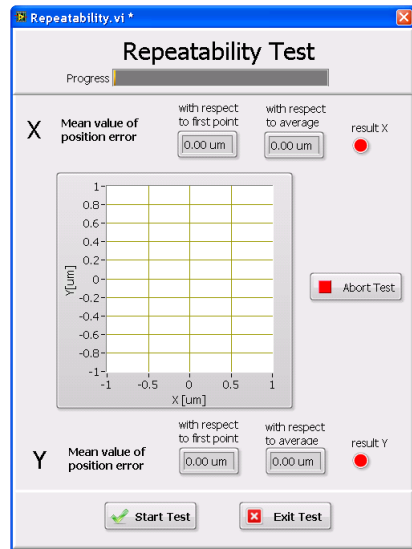


Fig. 5.32: UI for repeatability test

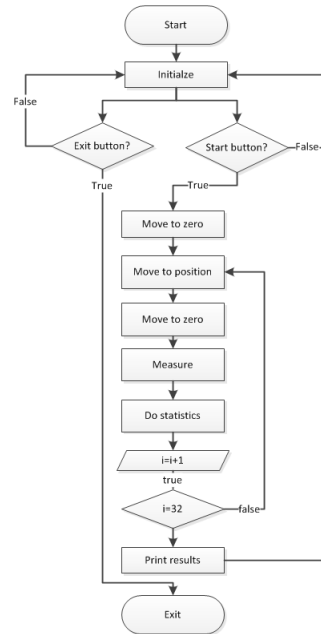


Fig. 5.33: Flow diagram for repeatability test

When the test is called, again the *Initialize* state occurs to set all values and controls to the proper value. After the start button is pressed, first the *Move to*

zero state moves the stage to the [0,0] coordinates and then the *Start* state is called, which starts the encoder data acquisition and fills in the queue with sequence of states. In state *Move to position* the stage moves to the one of the position specified in chapter 3.2 and back to to zero position. Then the *Measure* state occurs where the reading from the X and Y encoder is saved into an array which is then processed in *Do statistics* state every iteration of the test flowchart. The repeatability value for each of axes is calculated as

$$repeatability[\mu m] = \mu \pm 3\sigma \quad (5.6)$$

μ is a mean value of the \tilde{x}_i , which is displacement measured by linear encoder between the initial zero position x_0 and the position x_i after the stage returns from the specified position:

$$\mu = \frac{1}{n} \sum_{i=1}^n (x_i - x_0) \quad (5.7)$$

σ is a standard deviation expressed:

$$\sigma = \sqrt{\frac{1}{n} \sum_{i=1}^n (\tilde{x}_i - \mu)^2} \quad (5.8)$$

The front panel is updated every iteration of the test with actual position error displayed numerically and graphically in XY graph. If the final repeatability value lies within the specification the axis passed the test. The numeric and string result is then passed to the *Print results* state where the html report is generated.

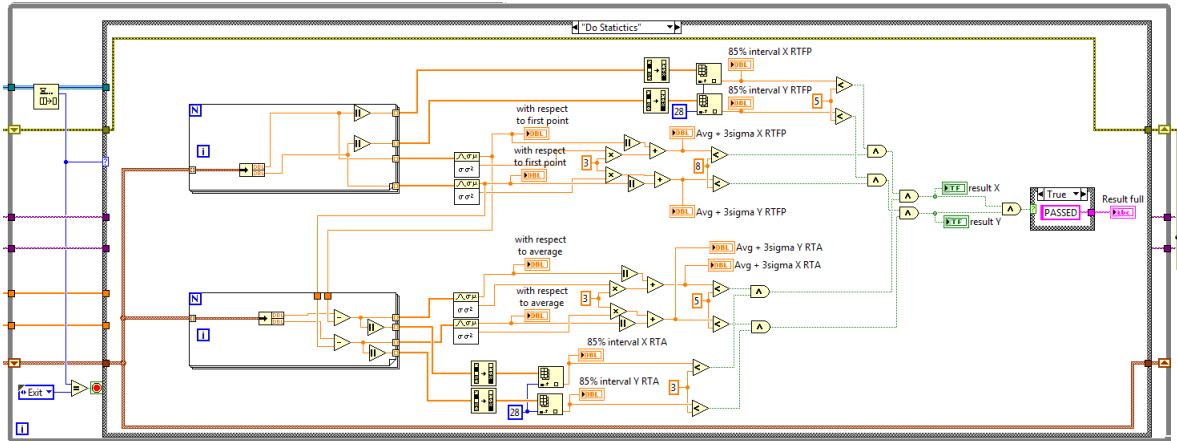


Fig. 5.34: *Do statistics* state

5.4.4 Smallest step test

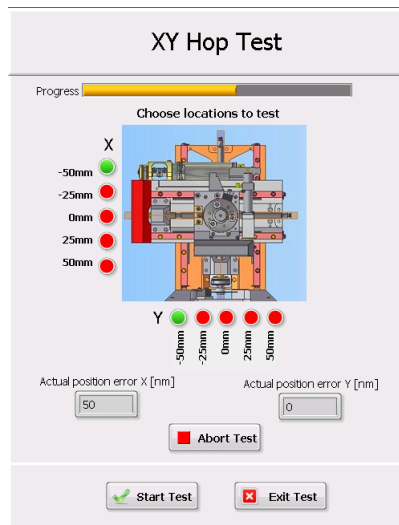


Fig. 5.35: UI for the smallest step test

The main feature of the smallest step test that has been implemented is that the user can now choose the locations where the test will be performed. For the first time the stage is assembled the test is performed for all the locations and based on the results for the particular locations the axis mechanism is adjusted and retested in locations which showed any irregularities. This is very time saving feature, because now the test can be performed on specified locations instead of running the whole test again. Choosing the locations is based on marking the boolean controls on the UI. Once set, the test is started by pressing the start button and the `choose_locations.vi` is called in the *Start* state. It reads the state of the boolean controls on the UI and based on its value it creates cluster containing the string name of the location, the numeric value with position of the location and the boolean value from which the axis mask for point to point move VI is derived.

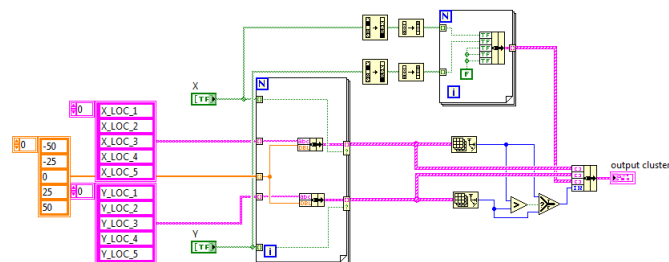


Fig. 5.36: `choose_locations.vi`

Next, the element in chosen location cluster is read by the `cluster_control.vi`. It is controlled by artificial variables Location and Position. Based on those variables the element in cluster is chosen describing the axis mask, name of the location and position and the numeric value describing where the location lies on the axis. When read, the axis moves to specified location and 10 moves with magnitude of 250nm in positive direction and 10 moves in negative direction are performed in *Measure* state. During every step, the displacement between initial and final position is read as from the rotational encoder on the axis so from the linear encoder. Those values are saved in the TDMS file, which is NI's file format for saving the measurement data in the structured form.

When measuring in first position is done, the stage moves by 0.2mm (which represents rotating the axis spindle by 90°) to next position and another 20 small steps are measured and saved. This way the test follows until all five positions at every of chosen locations are measured as described in 3.1. The data for every location are processed in *Print result* state. For every smallest step the position error is calculated as an difference between the commanded step (250nm) and real measured value. Those values are displayed in two graphs accompanied with string indicator if the position passed the test and with the maximum value of the error.

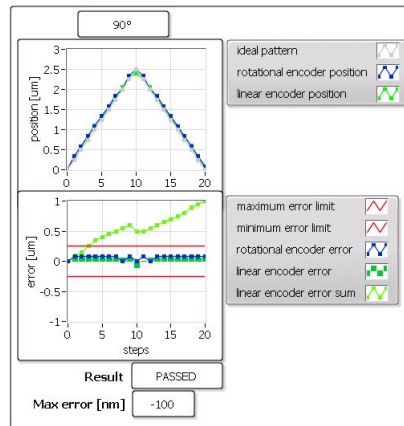


Fig. 5.37: Result graph for smallest step test - single position

5.4.5 Drift test, Burn-in test

As all the tests share the same programming pattern, it would be redundant to enter up thoroughly the dataflow, therefore only the UI and flow chart describing order of the states for state machine will be shown.

Drift test - after initialization and start the stage moves to the coordinate $[X,Y]=[0,0]$ and tilts to 52° . Then the Y axis performs point to point move to -1mm, then 1mm and finally back to 0mm. Once done, the stage settles for one minute and then the data acquisition from linear encoder on the Y axis starts measuring any displacement for 30 minutes. The UI is updated with absolute value of the Y drift in the waveform chart and the value of the drift divided by the time elapsed. After the time is out the html report is printed with the value value of the drift in time and if the result meets the specification.

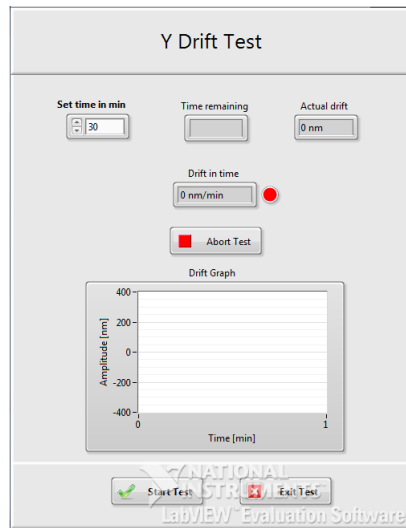


Fig. 5.38: UI for drift test

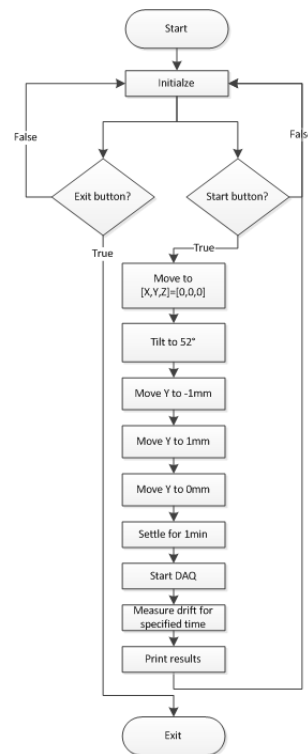


Fig. 5.39: Flow diagram for drift test

Burn-in test - This test serves to break in the stage's mechanism for all axes. After the initialization and start the stage moves with chosen axes within their limits for specified time.

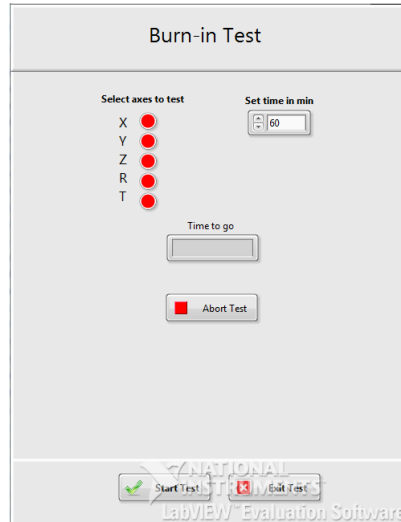


Fig. 5.40: UI for burn-in test

5.5 Test tool verification and evaluation

When the mechanics and software has been developed, it was necessary to verify that the linear and rotation precision test gives the correct results and the chosen reversal method is suitable for the test tool. Great advantage of the reversal method is that its result consist as of the motion error so that of the artifact profile. Therefore the simplest way to decide whether the results from the test tool are correct is to compare the artifact profile measured by the test tool with data gathered from the professional surface profile measurement tool. The data from the measurement has been provided in form of graphical illustration as well as the raw data which were then imported into the LabView environment and processed.

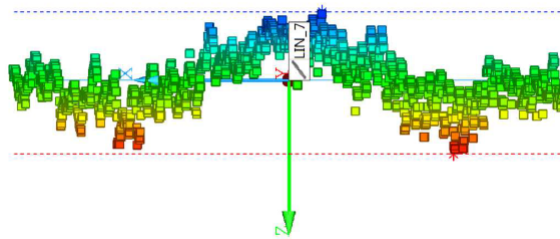


Fig. 5.41: Measured linear artifact profile by DII

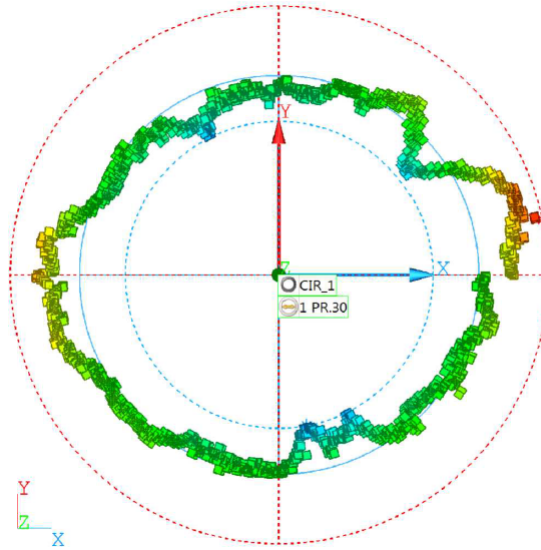


Fig. 5.42: Measured rotational artifact profile by DII

Then the test for linear and rotational precision has been performed and the data containing the artifacts shapes has been saved and plotted together with the data measured by the external supplier. As can be seen, comparison for the linear artifact showed that the biggest difference measured is $0.37 \mu\text{m}$. For the rotational artifact it can be clearly seen that both methods reveal the same disturbances on the profile and the biggest difference in amplitude is $2.6 \mu\text{m}$. The reason why the maximum difference in rotational measurement is almost ten times bigger than in linear case, can be attributed to the mechanical damage of the artifact as well as to little bit different location where the profile has been measured.

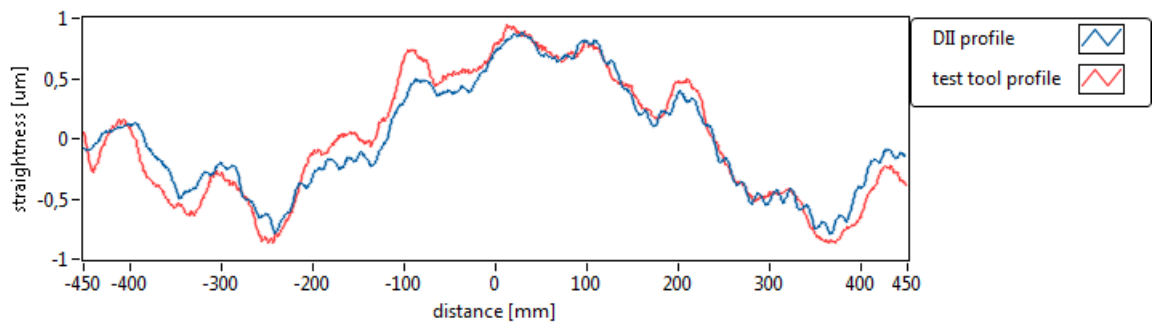


Fig. 5.43: Comparison of the linear artifact profile measured by test tool and by the external supplier

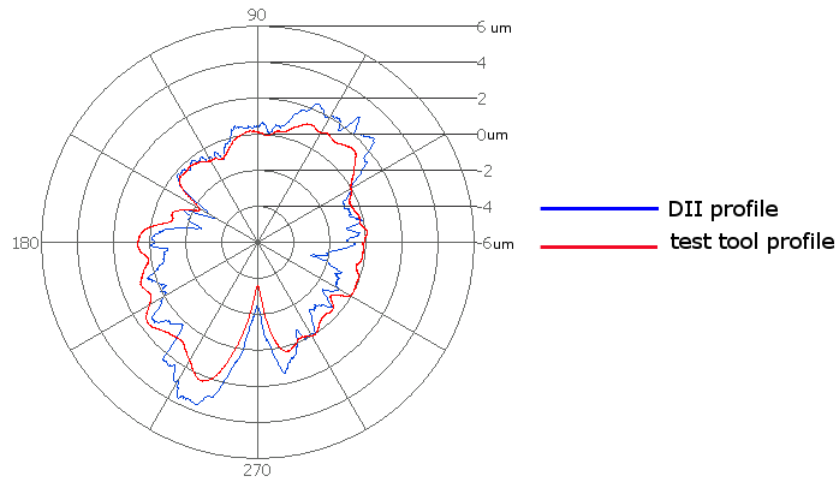


Fig. 5.44: Comparison of the rotation artifact profile measured by test tool and by the external supplier

Taken in mind the stated probe uncertainty of $2\mu\text{m}$ ([14]), the reversal measurement method for the linear and rotational precision test can be considered as valid. After all it must be emphasized that using this method extraordinary results have been achieved with equipment costing minimum compared to the LARA system.

The time taken for each of the tests must be also taken in consideration. The Repeatability, Burn-in, Drift, Linear and Rotational test time cannot be much influenced as every step of the testing procedure is more or less fixed. Yet in case of Smallest step great time save can be achieved. As mentioned in 5.4.4, now the user can choose e.g. only one location to be tested, therefore he does not have to run the whole procedure. It is save to say that this feature can save hours, as the adjusting the stage to pass the smallest step test is very slow process often taking several hours.

Table 5.1 show approximate time needed to perform particular test procedures including the preparation time needed for example to mount and reverse the artifacts.

PROCEDURE	TIME
Repeatability test	7 minutes
Smallest step test	30 minutes
X, Y linear precision test	20 minutes for each axis
R precision test	15 minutes

Tab. 5.1: Time needed to perform particular test procedures

The test tool application is provided to the supplier in form of .exe application. In order to properly run it, LabView 2012 Runtime Environment has to be installed on the test tool computer. Finally, the whole testing application has been thoroughly tested during the programming to ensure that it is user friendly, that it can be correctly ended even during the test and so that all controls are immediately responsive to the user interaction. What is more, during the testing not a single crash of the application has occurred and it is more than likely that application proposed in this thesis will replace the existing Matlab version with great appreciation.

6 CONCLUSION

The aim of this thesis was to create complex application which will test important mechanical parameters of 110x110mm stage mechanism for electron microscope at the manufacturer site. In the first part the basis of the electron microscopy has been proposed together with detailed description of the 110mm stage and its parameters.

In chapter 3 testing procedures which are performed on the stage are described with the explanation why and how they are used. Next, the used measuring equipment needed to obtain desired measurement values is introduced as well as the microscope software and hardware and their synergy is proposed.

The main part of the thesis deals with design of the mechanical parts needed for the testing procedures and programming of the testing application. At the end the verification of the reversal method used is shown to prove that the chosen method and its results are suitable for the newly implemented tests. Also the main characteristics of the new testing device are proposed.

All goals of this thesis were reached and the first part of the test tool containing the Smallest step test, Burn-in test and Repeatability test has been implemented and well appreciated at the manufacturer site. The addition of the Linear and Rotation precision test will be implemented in the third quarter of the year 2013.

BIBLIOGRAPHY

- [1] FEI COMPANY, *All you wanted to know about electron microscopy*, 2006
- [2] BARETT RESEARCH GROUP, *Nanotechnology: A brief overview*, [online], cit. 14-1-2013, dostupné z URL: <<http://barrett-group.mcgill.ca/tutorials/nanotechnology/nano02.htm>>.
- [3] FEI COMPANY, *FEI Company products*, [online], cit. 14-1-2013, dostupné z URL: <<http://www.fei.com/products/>>.
- [4] FEI COMPANY, *CRS New SEM stage v1.0 accepted*, 2010
- [5] DONALDSON, R.R., *A simple method for separating spindle error from test ball roundness error*, CIRP-Annals, Vol. 21, No.1, pp.125-126, 1972
- [6] EVENS, C.J., HOCKEN, R.J., ESTLER, W.T., *Self-calibration: reversal, redundancy, error separation and absolute testing*, CIRP-Annals, Vol. 45, No.2, pp.617-634, 1996
- [7] MARSH, E.R., *Precision spindle metrology*, Destech Publications, Inc., ISBN 978-1-60595-003-7, 2008
- [8] FEI COMPANY, *Mechanical user manual LARA v5*, 2008
- [9] VAŠKE, F., *Design and implementation of testing device for gonio mechanisms*, Brno, 2012, Brno University of Technology
- [10] MICRO-EPSILON, *Manual capaNCd 6100*, [online], cit. 14-1-2013, dostupné z URL: <<http://www.micro-epsilon.com/download/manuals/man-capaNCDT-6100-de-en.pdf>>.
- [11] MICRO-EPSILON, *Catalog capaNCd*, [online], cit. 14-1-2013, dostupné z URL: <<http://www.micro-epsilon.com/download/products/cat-capaNCDT-en.pdf>>.
- [12] FEI COMPANY, *RG2 Optical linear encoder*, [online], cit. 14-1-2013, dostupné z URL: <<http://www.renishaw.com/en/rg2-optical-linear-encoder-6441>>.
- [13] BOSCH REXROTH GROUP, *Excellence in motion control*, 2008, dostupné z URL: <<http://www.boschrexroth.com/>>.

- [14] WENZEL, *Co-ordinate measuring machines LH 54, LH 65, LH 87*, [online], cit. 28-1-2013, dostupné z URL: <http://www.wenzelamerica.com/brochures/DataSheet_LH54LH65LH%2087Standard.pdf>

LIST OF FIGURES

2.1	SEM and TEM microscope principle [2]	12
2.2	Examples of the FEI Company portfolio [3]	12
2.3	50x50mm stage driven by DC motors	13
2.4	100x100mm stage driven by piezo motors	13
2.5	The 110x110mm stage assembled	14
2.6	RY unit	15
2.7	X unit	16
3.1	Locations on each axis where the smallest step is measured	19
3.2	Repeatability moves [9]	20
3.3	TEM lamella preparation [4]	21
3.4	LARA measurement system for UHR stage [8]	22
3.5	Setup for forward (left) and reverse (right) spindle measurement [7] .	23
3.6	Graphical illustration of raw data, synchronous and asynchronous error [7]	24
3.7	Setup for forward (left) and reverse (right) linear measurement	24
4.1	Scheme of guard ring capacitor [10]	25
4.2	CapaNCDDT 6100 controller [11]	26
4.3	Signal change for various target geometries for CS02 sensor[11]	27
4.4	Placement of the linear encoders for X and Y axis	27
4.5	RG2 optical scheme [12]	28
4.6	Readhead RGH25F, RG2 20µm pitch scale, interpolator REF0400 [12]	29
4.7	Motion test tool at FEI R&D	29
4.8	TAD	31
4.9	Test tool connection scheme	31
4.10	NYCe4000 motion controller	32
5.1	Capacitive sensor holder assembly	33
5.2	Capacitive sensor base with all possible sensor positions	34
5.3	Base with capacitive sensor holder	34
5.4	Linear artifact	35
5.5	Supports for linear artifact	35
5.6	Linear artifact adjustment mechanism	35
5.7	Setup for linear measurement on X axis	36
5.8	Rotational artifact and tightening knob	37
5.9	Rotational measurement setup	37

5.10	Connection to the MotionServer in LabView	38
5.11	Reading the stage states in LabView	38
5.12	Moving the stage in point to point mode in LabView	39
5.13	Main UI of the test tool application	40
5.14	Initializing the queue	41
5.15	Adding elements into the queue - producer loop	41
5.16	Calling the test VI - consumer loop	42
5.17	Complete block diagram for Main.vi	43
5.18	UI for rotation test	44
5.19	Flow diagram for rotation test	44
5.20	Filling in the queue with test procedures	44
5.21	Instruction window	45
5.22	<i>Do settle moves</i> state	45
5.23	<i>Measure</i> state	46
5.24	Raw measured data	46
5.25	Best sine fit extrapolated from raw measurement	47
5.26	Raw displacement - sum of motion and artifact error	47
5.27	<i>Do statistics</i> state	47
5.28	<i>Print results</i> state	48
5.29	Rotation test html report	48
5.30	Approaching the linear artifact	49
5.31	<i>Measure</i> state	50
5.32	UI for repeatability test	51
5.33	Flow diagram for repeatability test	51
5.34	<i>Do statistics</i> state	52
5.35	UI for the smallest step test	53
5.36	choose_locations.vi	53
5.37	Result graph for smallest step test - single position	54
5.38	UI for drift test	55
5.39	Flow diagram for drift test	55
5.40	UI for burn-in test	56
5.41	Measured linear artifact profile by DII	56
5.42	Measured rotational artifact profile by DII	57
5.43	Comparison of the linear artifact profile measured by test tool and by the external supplier	57

5.44 Comparison of the rotation artifact profile measured by test tool and
by the external supplier 58

LIST OF TABLES

2.1 Specification for 110mm stage 16

3.1 Number of stages delivered in particular years 17

3.2 Stage issues 18

5.1 Time needed to perform particular test procedures 58

LIST OF APPENDICES

On appended CD

1. **Datasheets** - ../datasheets folder
 - Renishaw RGH25F Encoder System
 - CapaNCDT 6100 Manual
 - CapaNCDT 6100 Catalogue
2. **Profile measurement protocols** - ../measured_profiles folder
 - Rotational artifact profile
 - Linear artifact profile